**Univerzita Karlova v Praze**
**Přírodovědecká fakulta**

Studijní program: Chemie
Studijní obor: Chemie v přírodních vědách


**Michal Trachta**

# Modelování ADOR syntézy nových zeolitů

# Modeling of Hypothetical Zeolites Based on the ADOR Process

Bakalářská práce

Vedoucí bakalářské práce: RNDr. Ota Bludský, CSc.

Praha 2014

**Prohlášení:**

Prohlašuji, že jsem závěrečnou práci zpracoval samostatně a že jsem uvedl všechny použité informační zdroje a literaturu. Tato práce ani její podstatná část nebyla předložena k získání jiného nebo stejného akademického titulu.

V Praze, 29.5.2014

Podpis

**Poděkování**

Tímto bych chtěl poděkovat svému školiteli RNDr. Otovi Bludskému, CSc. za odborné a trpělivé vedení při tvorbě této práce. Dále bych chtěl poděkovat rodičům za podporu při mém studiu na vysoké škole.

# Abstrakt

Zeolity jsou materiály s širokým uplatněním v průmyslu. Jsou schopny katalyzovat nejrůznější reakce, stejně tak mohou být použity jako molekulová síta nebo adsorbenty. Řízený design zeolitů je důležitým cílem chemiků, úplná kontrola nad porézností a složením zeolitů může vést k vývoji optimálních materiálů pro dané použití.

V nedávné době byla navržena a úspěšně aplikována nová strategie syntézy zeolitů. Tato strategie, nazývaná ADOR proces, může vést k syntéze mnoha nových materiálů s definovanou strukturou a porézností. V této práci jsou zkoumány struktury hypotetických zeolitů, k jejichž syntéze by ADOR proces mohl vést, a je zde brána v potaz realizovatelnost jejich syntézy. Syntéza zeolitů z lamelárních prekurzorů, která je základem ADOR procesu, se tak může v budoucnu stát široce rozšířenou technikou.

Klíčová slova: ADOR proces, hypotetické zeolity, teoretický výzkum

# Abstract

Zeolites are materials with a large variety of applications in industry. They are able to catalyze many types of reactions and can be used as molecular sieves or adsorbents. Tailored design of zeolites is an important goal for chemists as the full control over zeolite porosity and composition can lead to optimal materials for industrial purposes.

Recently, a new strategy for the zeolite synthesis was proposed and successfully applied for several systems. This strategy, called ADOR, can lead to synthesis of many new materials with a defined structure and porosity. The synthesis of new zeolites from lamellar precursors, which is in the heart of the ADOR process, may become widely used technique in the near future. In this work we focus on hypothetical products of the ADOR process and address the relationship between their structure and feasibility of their synthesis.

Keywords: ADOR process, hypothetical zeolites, in silico investigation

# Contents

**Acronyms** **vi**

**1. Introduction** **1**

**2. Methods** **7**

2.1. Density Functional Theory 7

2.2. Force Fields 10

2.3. Computational Details 12

**3. Modeling of the ADOR Process** **13**

3.1. Models and Approximations 13

3.2. Synthesis Feasibility Criteria of Zeolites 15

3.3. Modeling of -D4R Materials 17

3.3.1. Organization and Reassembly Process 17

3.3.2. Hypothetical -D4R Zeolites 21

3.4. Modeling of -S4R Materials 24

3.4.1. Organization and Reassembly Process 24

3.4.2. Hypothetical -S4R Zeolites 26

**4. Conclusion** **31**

**5. References** **32**

**Appendix A – Supplementary Data** **35**

**Appendix B – CD Content** **45**

# Acronyms

| | |
|---|---|
| -D4R | hypothetical zeolite with lamellae connected by oxygen linkers |
| -S4R | hypothetical zeolite with lamellae connected by S4R linkers |
| ADOR | process/strategy used for synthesis of new zeolites (assembly, disassembly, organization, reassembly) |
| CS | coordination sequences |
| D4R | double four-membered ring unit in zeolites |
| DFT | density functional theory |
| FD | framework density |
| FE | framework energy |
| FF | force field |
| LID | local interatomic distances |
| PBE | DFT functional of Perdew-Becke-Ernzerhof |
| S4R | single four-membered ring |
| SDA | structure directing agent |
| SLC | Sanders-Leslie-Catlow potential |
| T-atom | atom with tetrahedral coordination in zeolite framework |
| vdW-DF2 | non-local van der Waals density functional |
| VS | vertex symbols |

# 1. Introduction

Zeolites are materials defined by the International Zeolite Association as:

> … aluminosilicates with open 3-dimensional framework structures composed of corner-sharing $TO_4$ tetrahedra, where T is Al or Si. Cations that balance the charge of the anionic framework are loosely associated with the framework oxygens, and the remaining pore volume is filled with water molecules. The non-framework cations are generally exchangable and the water molecules removable. This definition has since been expanded to include T-atoms other than Si and Al in the framework, and organic species (cationic or neutral) in the pores.[1]

Some zeolites can be found in nature in volcanic rocks and deep-sea sediments.[2] Most of the zeolites frameworks, however, were synthesized. Until now 218 unique zeolite frameworks were confirmed by International Zeolite Association – Structure Commission.[1] The diversity of the zeolite frameworks is a consequence of a large number of the building units.

The most common synthesis of the zeolites uses the hydrothermal process, in which the T-atom source is treated in hot alkaline aqueous solutions. Si and Al are the most common T-atoms in zeolites, but other elements, such as Ge, P, B, etc., can be used as well.[3,4] The ratio of these agents may vary and thus influences the composition of the final material to some extent. Moreover, the structure directing agent (SDA) or agents are added to the reaction mixture. This compound arranges the T-atom-containing molecules by its steric and electrostatic effects and thus helps to organize the structure. The material is obtained after hours or days of treatment in autoclave at high temperatures.[5] To remove the SDA the calcination process is performed. Additionally the calcination can also cause the condensation of remaining silanol groups. Thus, the zeolite itself can be formed after calcination rather than after the hydrothermal synthesis – one special case will be discussed later. The conditions used during the synthesis influence the T-atom ratio, impurities and defects in the zeolite.[3] It should be pointed out that the conditions determine also the framework type. As a result a mixture of more different zeolites is obtained A great effort thus has to be made to optimize the synthesis conditions.

The zeolites have many applications in industry and their importance is continuously increasing. They are used for their catalytic, adsorption, molecular sieve-like and cation exchange properties. Their catalytic properties make them very important, e.g. in the field of oil refinery and various chemical processes (such as alkylation, isomerization, epoxidation)[6] can be catalyzed. A wider expansion of applications is slowed down by our inability to fully tailor the properties of these materials and to decrease their production costs. Properties, such as framework density, pore size and accessible volume, are determined by the framework type. The T-atoms in the zeolites affect the distribution of electron density and thus influence their catalytic properties. In particular, the Al content introduces negative charge to the rest of the framework which is compensated by hydrogen atoms. These hydrogen atoms are released in the water environment as hydrogen cations, thus the Al content results in increased acidity of the zeolite. The size and accessibility of the pores (or cavities) and the acidity of the zeolites are aspects which need to be optimized to develop an optimal catalyst for a desired purpose. The acidic properties of the zeolite depend mostly on the Al content (usually described as Si/Al ratio) and the Al positions in the material. In most cases Al is located randomly in the zeolite, but some exceptions were reported.[7] As was already mentioned, the size of the pores is determined by the framework type. However, there are post-synthesis methods to increase the pore size and the accessibility (i.e. desilication) and modify the reactivity (i.e. post-synthesis substitution of T-atoms, surface modification).[4] Unfortunately, this often leads to irregular product without well-defined properties and zeolite-related materials (zeotypes) are obtained.

It has been found that some zeolites are prepared (or can be prepared) through lamellar precursors. After hydrothermal synthesis ordered lamellae are obtained and these lamellae are interconnected during the calcination process, when the condensation of silanol groups occurs. These lamellae, often called two-dimensional zeolites (2D zeolites), have some interesting properties. They are periodic in two dimensions, in contrast with the normal three-dimensional zeolites (3D zeolites). In addition, 2D zeolites have silanol groups located on the surface and more flexible framework resulting in a different chemical behavior. The main advantage of 2D zeolites is the accessibility of substrate molecules which can be further enhanced by different techniques, such as pillaring, synthesis of disordered materials, etc.[8] Access to the lamella is much easier than access through channels of 3D zeolites. On the other hand, 2D zeolites have a lower shape selectivity, because the lamella is more or less flat, in contrast with complex channel systems in 3D zeolites. Obtaining 2D zeolite as a lamellar precursor in 3D zeolite synthesis is not the only way of preparing such materials.[9] 2D zeolite

can be also prepared by synthesis, where the growth in one direction is stopped by the use of surfactant molecules. Moreover, 2D zeolite can be a product of decomposition of 3D zeolite (top-down approach).

*ADOR Process – Way to New Zeolites*

2D zeolites obtained by decomposition of 3D zeolites were found to be possible precursors for synthesis of new zeolites. The whole procedure of synthesis and transformation of one 3D zeolite into another over a 2D intermediate product is called the ADOR (assembly, disassembly, organization and reassembly) process (see Figure 1). In this process the parent zeolite is synthetized, dissembled and finally the lamellae are obtained.[10] The lamellae are organized (e.g. using the SDA) and then reassembled through the calcination process. From this description immediately follows the requirement for the structure of the parent zeolite. The framework must be virtually composed of lamellae connected just by removable linkers. It was shown that the double four-membered ring (D4R; a cube with silicon atoms in vertices and oxygen atoms on edges) building unit in germanosilicate zeolites fulfills the condition for the removable linker. The zeolites satisfying the framework and composition conditions (and containing the D4Rs) are ITH, ITR, IWR, IWV, IWW and UTL. For the UTL case, the ADOR process was already successfully performed and new zeolite, PCR (originally called IPC-4), was synthesized.[11]

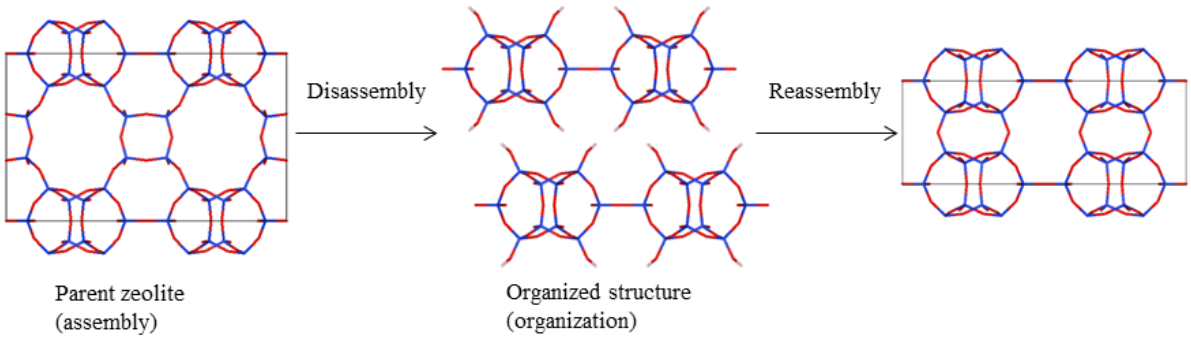


**Figure 1.** ADOR process scheme (oxygen atoms depicted red; VESTA program[12] used for structure visualizations).

D4R composite building unit seems to have significant importance in the ADOR process. It is a common structure element in many large-pore and extra-large-pore zeolites,[13,14] because the very compact units, such as the D4R unit, are related with the possibility of forming large pores. Due to its bend angles the D4R is a strained structural motif and consequently has a lower stability. It is one of the structure elements formed in reaction mixtures in the prenucleation phase,[13] the formation of D4R units can be enhanced by addition of Ge atoms. The germanium atoms build into the D4R and stabilize the unit, the germanium content in the rest of the zeolite is usually noticeably smaller.[15,16] The calculations suggest that among the D4R units with various number of Ge atoms that which has three Ge atoms is the most stable,[13] but various numbers of Ge atoms were observed.[15] Due to the content of germanium the D4R unit is sensitive to hydrolysis.[14]

One interesting feature of the ADOR process is a possibility to prepare new zeolites from a single parent zeolite (see Figure 2). In the organization phase of the ADOR process the lamellae could be arranged in many ways – different relative positions of the lamellae can lead to different zeolites or irregular products. The organization itself proceeds via formation of interlamellar hydrogen bonds between the surface silanol groups. Their formation might be affected by the presence of a proper SDA which are thus able to direct the synthesis of various zeolite frameworks. Although preparation of more zeolites by lamellae rearrangements was not achieved by the ADOR process yet, it can be illustrated on the example of the FER and CDO zeolites, which are formed by different arrangements of the same lamellae.[17] After the rearrangement the FER-type material was prepared from CDO precursor RUB-36,[18] however combination of swelling, deswelling and proper SDA was necessary, indicating that this kind of synthesis can be a tough problem. Notice that FER has about 2 kJ/mol lower framework energy than CDO (computed using Sanders-Leslie-Catlow potential – for details see Methods; for definition of framework energy see section 3.2) so this lamellae rearrangement is energetically favored.

Another way of the modification of the framework can be performed using silylation agent added to the organization phase. This results in building additional silicon atoms into the framework. For the UTL zeolite, this synthesis was already performed with diethoxydimethylsilane as the silylation agent which leads to the formation of single four-membered rings (S4Rs; four silicon atoms and four oxygen atoms forming a ring) interconnecting the lamellae and thus expansion of the interlamellar space and the pore size (with respect to IPC-4) is observed. The resulting material is called IPC-2.[11]

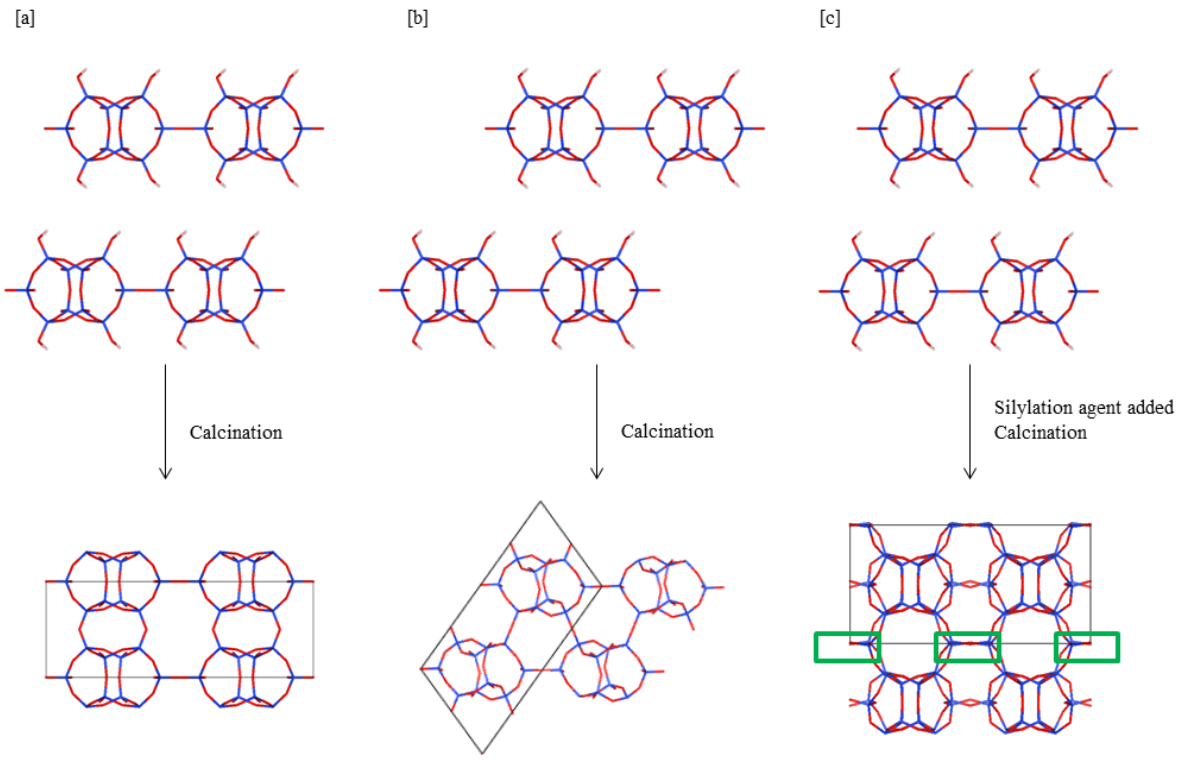


**Figure 2.** Organization and reassembly phase of the ADOR process. [a] The lamellae in the organization phase and in the final material are in the same relative positions as in the parent zeolite (except the interlamellar distance and small shift due to hydrogen bonds). In this work, we called this a "fundamental arrangement". [b] An alternative arrangement with relative shift between the lamellae in one or two directions. [c] Silylation agent added. This is also a fundamental arrangement, but in this case the lamellae are connected in the final material by S4R linkers (marked by green rectangle) and not oxygen linkers as in the previous cases.

An alternative to the ADOR process is the inverse σ transformation (a selective removal of some T-atoms, in this case layers of T-atoms). Also this transformation was already performed for UTL zeolite. In this process the S4R layer (half of the D4Rs) is removed and the interrupted framework is connected through the calcination process leading to a new material called COK-14,[19] which should have the same topology as IPC-2 (OKO framework type). Although the inverse σ transformation and the ADOR process have some similar features (i.e. both use the instability of D4R composite building unit), the inverse σ transformation leads directly to the S4R-connected material, whereas the ADOR process in principle allows synthesis of a larger variety of zeolite structures. Unfortunately, the feasibility of the ADOR process still remains an open question. Recently, the IWW germanosilicate was stabilized by the ADOR process – the Ge-rich D4R units were removed and then restored by addition of silylation agent, increasing thus the Si/Ge ratio in the resulting material while keeping the same framework topology.[20] This might be indication that the parent IWW zeolite is preferred over the ADOR-derived structures without D4R units and their synthesis can thus be difficult.

In silico design of new zeolites has attracted a considerable interest of computational chemists in the past decades. Millions of hypothetical zeolite structures have been predicted and stored in various web-based databases.[21,22] While a large number of zeolite structures are shown to be thermodynamically accessible, the actual synthesis routes remain unknown. In this work we use a different approach – we try to generate all feasible zeolite structures derived from a given parent material using a known synthesis protocol. The synthesis feasibility of hypothetical zeolites is evaluated using various criteria proposed previously, e.g. by means of a feasibility factor[23] or local interatomic distances (LIDs).[24] This strategy has many advantages over the standard brute-force approach. First, we closely follow existing synthetic route which increases the probability that at least some of the predicted structures will be synthesized in the near future. The structural information and calculated diffraction patterns can help to identify the synthesis products. Second, we deal with a limited number of structures (compared with a number of hypothetical structures in zeolite databases) which allows us to employ a more reliable level of theory. The use of non-empirical methods for geometry optimization of several hundreds of zeolite structures is computationally very demanding task. Thus, to assess reliability of affordable empirical predictions the calculated ab initio results are compared with those obtained by the Sanders-Leslie-Catlow potential[25,26] for all investigated zeolites.

# 2. Methods

## 2.1. Density Functional Theory

Using the modern quantum-chemistry methodology, the non-relativistic electronic Schrödinger equation,

$$\hat{H}\Psi = E\Psi \tag{1}$$

is solved to obtain the electronic energy $E$ and the wavefunction $\Psi$. Since most *ab initio* methods are unable to solve the N-electron problem exactly, some approximations have to be made. The Hartree-Fock method, the starting point of many high-level *ab initio* methods, treats the electron-electron repulsion in an averaged way leading to error in energy since the motion of electrons is not correlated (the averaged model cannot account for avoiding of the two electrons due to repulsion). This difference in energy is called the correlation energy and is defined as follows

$$E_{non-relativistic} = E_{HF-limit} + E_{corr} \tag{2}$$

In the equation (2), $E_{corr}$ is the correlation energy, $E_{non-relativistic}$ is the exact energy without considering the relativistic effects and $E_{HF-limit}$ is energy computed on the Hartree-Fock level with an infinite basis set. Notice that the correlation energy is always negative. Although the post Hartree-Fock methods (such as the Møller-Plesset perturbation theory or Configuration Interaction) are able to cover the correlation energy, they are not accurate enough or their computational cost is extremely high. Considering the problems of the standard ab initio methods briefly highlighted here, it is obvious that a search for more efficient approaches is needed. The density functional theory (DFT) approaches use electron density instead of electronic wavefunctions. The relation between wavefunction and electron density is

$$\rho(\vec{r}) = N \int \dots \int |\Psi(\vec{x}_1, \vec{x}_2, \dots, \vec{x}_n)|^2 ds_1 d\vec{x}_2 \dots d\vec{x}_N \,. \tag{3}$$

The electron density $\rho$ depends on the spatial coordinates and the integration/summation runs over all spatial and spin coordinates of $N$ electrons except one electron spatial coordinates. As was shown by Hohenberg and Kohn, the ground-state electron density contains sufficient

information to compute the energy (H-K theorems state that the energy functional exists and the variational principle applies). The Hamiltonian in Schrödinger equation (the Born-Oppenheimer approximation was used) can be separated into following terms,

$$\hat{H} = \hat{T} + \hat{V}_{ee} + \hat{V}_{Ne} \tag{4}$$

and so can be the energy functional,

$$E[\rho] = T[\rho] + E_{ee}[\rho] + E_{Ne}[\rho]. \tag{5}$$

Here the first term represents the kinetic energy, the second is energy contribution due to electron-electron repulsion and the third is nucleus-electron attraction and has a very simple form (notice that atomic units are used for simplicity),

$$E_{Ne} = \int \rho(\vec{r}) V_{Ne} d\vec{r} \tag{6}$$

where $V_{Ne}$ is the coulombic potential caused by the presence of atomic nuclei. The exact form of $T$ and $E_{ee}$ functionals remains unknown, together they are referred as the Hohenberg-Kohn functional ($F_{HK}$). In contrast with the $E_{Ne}$ functional, these two functional should have universally valid form independent of the system. Although the precise form of the two functional is not known, approximations can be made. The $E_{ee}$ functional is usually divided into classical Coulombic electron-electron repulsion term $J$ and a non-classical correction term $E_{ncl}$ accounting for the exchange and Coulomb correlation and removing the self-interaction

$$E_{ee}[\rho] = J[\rho] + E_{ncl}[\rho] = \frac{1}{2} \int \int \frac{\rho(\vec{r}_1)\rho(\vec{r}_2)}{r_{12}} d\vec{r}_1 \, d\vec{r}_2 + E_{ncl}[\rho] \tag{7}$$

Here $r_{12}$ is the distance between electrons 1 and 2. The exchange correlation is consequence of the Pauli principle, the Coulomb correlation is caused by Coulombic repulsion. Both effects are reflected in DFT as additional potentials and are called Fermi and Coulomb holes, respectively, because each electron is surrounded by a space where probability of presence of other electrons is lowered. Note that the Fermi hole usually takes care of the self-interaction problem. Together they form exchange-correlation hole; this concept has a physical meaning, in contrast to the separated holes.[27] Unfortunately, the attempts to find functional for kinetic energy failed and the approximations doesn't have desired accuracy, so Kohn and Sham decided to use different approach. They defined the non-interacting reference system, which

has the same electron density as the interacting one, and computed kinetic energy for it. For this reason the orbital model and wavefunction in the form of Slater determinant were adopted. The correction of kinetic energy between the non-interacting and real system was added to the exchange-correlation term. The functionals $J$, $V_{Ne}$, and $E_{XC}$ (exchange-correlation hole + kinetic energy correction) give together external potential needed for the non-interacting reference system.

The basic concepts of DFT were shown above. It is obvious, that the last thing needed for application of DFT is the exchange-correlation functional (containing the effects of exchange correlation, Coulomb correlation, kinetic energy and self-interaction correction). Various approaches to obtain approximate form of this functional will be outlined here. To this point, all DFT functionals depended just on the value of electron density in certain point of space. This approach is called the local density approximation (LDA). The form of exchange and correlation functionals is based on the model of uniform electron gas. LDA is a starting point for another DFT branches. To improve performance, the dependence on gradient of electron density was added into the exchange-correlation functional. This is the gradient expansion approximation (GEA). Surprisingly, GEA doesn't perform well, because it violates some rules the exchange-correlation hole must satisfy.[27] In reaction to this fact, the generalized gradient approximation (GGA) was developed. These methods are based on GEA, but the rules for exchange-correlation hole are satisfied. One of the GGA functionals was made by Perdew, Burke and Ernzerhof (PBE),[28] this functional is used in this work.

The gradient of electron density describes somehow the density in close neighborhood. If we go to extreme, for every point the information about the whole density may be available. In this moment, the functional is not local anymore. Such functionals are called nonlocal. The nonlocal functionals are able to account for dispersion effects (in fact long-range Coulomb correlation effects), because the electron density in one place feels the presence of electrons in other – even distant – places. This is very hard to reflect in the LDA, GEA and GGA (all of these are local). In this work the second version of the van der Waals density functional[29] (vdW-DF2) was used for calculations including dispersion effects. The vdW-DF2 functional consists of rPW86 exchange (GGA) and nonlocal correlation functional (LDA correlation + nonlocal vdW).

## 2.2. Force Fields

The ab initio and DFT methods are computationally expensive. In cases of very large systems the time or hardware requirements could be so high, that the use of these methods is completely impossible. Then the use of simpler approach is needed, the semi-empirical and empirical methods can be used. We will now focus on the force fields (FF), which are the empirical methods and have the greatest timesaving factor. The force fields are obtained as a generalization of computational and/or experimental data. The potential energy is described as a function of the nuclei positions, where the overall potential is formed as a sum of various contributions. The potential can be divided to two main parts – covalent and non-covalent, which can be further divided to single terms. Some simple force fields represent the covalent part as a contribution of bond stretching, angle bending and torsion terms. In more complex approaches the coupling between these degrees of freedom is added (i.e. bond-bond term for neighbouring bonds sharing common atom, bond-angle term, angle-angle torsion term, etc.). Moreover, other potentials and constraints (i.e. the out of plane contribution as a planar constraint) might be added. The non-covalent part is formed by the Coulomb interaction and the van der Waals (vdW) interaction. The van der Waals interaction is usually expressed as Lennard-Jones potential. The Coulomb interaction needs the charges to be specified. The charges are usually fixed for every atom type, but they could even be geometry-dependent. To increase the accuracy of the force field the polarisability could be taken to account. The polarisability may be expressed using a polarisability constants or it could be described using the shell model (for more details see GULP[30] manual), where the atom is divided to core (which represents nucleus and core electrons) and shell (which represents valence electrons). The core and shell can move separately, but they are connected using a distance-dependent potential. The accuracy of the force field depends on many factors. The most important aspects are the size of the data set, appropriate and numerical stable parametrization and good results in the transferability test. Of course, proper use of the force field is crucial for reliable results.

Sanders-Leslie-Catlow potential[25] (hereinafter referred to as SLC potential) is a potential used for modeling of zeolites. In this work we used its slightly modified version, which is defined in the article of Schöder et al[26] and which is implemented in the GULP program.[30] This force field consists of Buckingham potential, Coulomb potential, angle term and core-shell polarization term (the latter just applied to oxygen atoms). Let's take a closer

look at the potential form. The coulombic interaction is responsible for the majority of potential energy and has the form

$$V_{Cou} = \frac{1}{4\pi\varepsilon_0} \times \frac{Q_1 Q_2}{r}. \quad (8)$$

Here $\varepsilon_0$ is vacuum permittivity, $Q_1$ and $Q_2$ are the charges of interacting particles and $r$ is the distance between them. For silicon the charge is 4.0, for oxygen the charges are 0.86902 and -2.86902 for core and shell (respectively; all charges are introduced as a multiple of the elementary charge). The Buckingham potential plays two important roles – in the short range it's the main repulsive term protecting the system from collapse due to Si-O coulombic attraction and it also accounts for dispersion,

$$V_{Buck} = A \times e^{-r/\rho} - Cr^{-6}. \quad (9)$$

The parameter $A$ is 1283.907 eV for Si-$O_{shell}$ interaction and 22764.0 eV for $O_{shell}$-$O_{shell}$ interaction (notice that there is no Si-Si term). The corresponding parameters $\rho$, which control the distance-dependent decrease of the potential, are 0.32052 and 0.149 Å, respectively. The dispersion is described using the $C$ parameter, which has the value 10.66158 and 27.88 eV·Å$^6$, respectively. The oxygen atom core and shell (both are charges) are connected by a harmonic spring,

$$V_{CS} = \frac{1}{2} kr^2. \quad (10)$$

In the equation (10), $r$ is the core-shell distance and the constant is equal to 74.92 eV·Å$^{-2}$. The angle bending is described using a harmonic potential,

$$V_{Angle} = k(\theta - \theta_0)^2. \quad (11)$$

The angle term is evaluated only for $O_{shell}$-Si-$O_{shell}$ angle, the constant is 2.09724 eV·rad$^{-1}$ and the non-bended angle $\theta_0$ is 109.47 °. In comparison with the previous potential terms this term has the smallest energy contribution.

### 2.3. Computational Details

The force field optimizations were performed using the General Utility Lattice Program (GULP)[30] with the SLC potential as is defined in the GULP libraries (catlow.lib file). Optimise, molq, phonon and nosymmetry keywords were used. Optimise keyword means optimization; in this work full optimizations (cell parameters and ionic positions) were performed. Molq keyword is used for computing coulombic interactions within the molecule (in our case the molecule is the zeolite material). Nosymmetry keyword turns off the symmetry and phonon calculation analyzes the optimized structure. If imaginary phonon mode is present, the structure is not fully optimized (it is not a minimum, just a stationary point). In the case of imaginary phonon mode (or modes), the symmetry were lowered with respect to the phonon calculation using the lower_symmetry keyword and then the structure was optimized again. To control the measure of disrupting the symmetry, the slower option was used. The optimal value of slower option depends on the negative phonon frequencies, too high value can destroy the structure – especially for large negative phonon frequencies. In most cases slower values of 0.01 and 0.03 were optimal. Sometimes was necessary to repeat the lower symmetry and following optimization procedure to obtain an energy minimum. In some cases the core-shell harmonic spring broke (exceeded limit distance) – sometimes the change of optimization algorithm helped (from BFGS to conjugate gradients) to avoid this problem. For some bad initial structures we were unable to optimize them using any procedure.

The PBE[28] and vdW-DF2[29,31] calculations were performed using the Vienna Ab-initio Simulation Package (VASP).[32] For all the calculations the PREC keyword (controlling the precision of computation) was set to high. The kinetic energy cutoff was set to 800 eV. Soft PAW/PBE pseudopotentials[33] were used with ENMAX values of 245 and 400 eV for silicon and oxygen, respectively. For all the calculations Γ-point sampling was used. The optimizations were performed with ISIF and IBRION tags set to 3 and 2, respectively, which means full optimization (cell shape and ion positions) using the conjugate gradient algorithm. The structures were considered optimized when all the forces are lower than 0.01 eV $Å^{-1}$.

# 3. Modeling of the ADOR Process

## 3.1. Models and Approximations

As was already mentioned in Introduction, the ADOR process can lead to a large (in principle infinite) number of structures from each suitable parent zeolite. In this work two main groups of the resulting structures with distinct interlamellar linkers were investigated, these groups are denoted -D4R and -S4R. The -D4R and -S4R refer to a kind of interlamellar liker between lamellae obtained from the parent zeolite. The -D4R material contains lamellae connected by oxygen (T-O-T) linkers corresponding to a complete removal of the D4R building units from parent zeolites while the -S4R material contains single four-membered rings (S4Rs) built up in place of the removed D4R units (not necessarily in the same position). We assume that the final product after calcination is a regular highly ordered material (typically formed by a single lamella per unit cell) and fully-condensed (no silanols left after the calcination process). The influence of SDA is not explicitly modeled, but the SDA effect is reflected indirectly in relative shifts between the lamellae with respect to their positions in the original material (parent zeolite). Also the water molecules were not modeled. Rotation of lamella is not taken into account. Moreover, all the zeolites are modeled as pure silica. When addition of silylation agent is modeled, only formation of S4R unit is considered.

The formation of zeolite is related to stability (energy) of the organized structure (system after the organization phase) and the height of the energetic barrier for the reaction. The energy of the organized system is determined mainly by the positions of silanol groups, because it's influenced mainly by forming of hydrogen bonds. We assume that this energy is strongly related with energy of the final zeolite, because the strain in the final material is reflecting the non-ideal relative positions of silanols and also the energetic barrier is probably higher for weaker (longer) hydrogen bonds. If we suppose that this is true, than by comparison of the zeolite energies we can predict the feasibility of the zeolite synthesis (and the preference of some zeolite structure with respect to another). Moreover, using this simplified scheme, it is not necessary to model the whole ADOR process with all its aspects, just all the possible final zeolites structures and their energies and other characteristics would be enough for analysis of reaction feasibility.

The structures of parent zeolites (ITH, ITR, IWR, IWV, IWW and UTL) were obtained from the Database of Zeolite Structures.[1] As this corresponds to the assembly in the ADOR process, the rest of the ADOR process was then modeled. The double-four ring units were removed and the disrupted bonds were terminated by hydrogen atoms. In this phase the lamellae were formed.

It should be pointed out some differences between the parent zeolites and the lamellae (see Table 1). From the investigated zeolites the ITR, IWV and UTL zeolites contains two lamellae interconnected by D4Rs in the unit cell. However, in the IWV and UTL cases the second lamella may be gained by translation of the first lamella, on the other hand the second lamella of ITR may be gained by flipping over and translation of the first lamella. From this analysis it's obvious, that ITR must be modeled as two lamellae in the unit cell, while the IWV and UTL can be modeled as one lamella in different unit cell (different shape and half of the original volume).

Another interesting thing is that ITH- and ITR- based lamellae have the same topology.[34] All the lamellae in this work have both sides topologically identical.

**Table 1.** Lamellae characteristics derived from the DFT-optimized parent zeolite parameters

| Parent zeolite | Lamella parameters[a] | | | Number of silanols[b] | Silanol density[b] | T-atom density | Channel through[c] |
|---|---|---|---|---|---|---|---|
| | [Å] | [Å] | [deg] | | [$10^{-3}$ Å$^{-2}$] | [$10^{-3}$ Å$^{-2}$] | |
| UTL | 12.5 | 14.1 | 90.0 | 4 | 22.5 | 169.1 | - |
| IWW | 13.1 | 42.5 | 90.0 | 16 | 28.8 | 143.9 | R12; R8 |
| IWV | 14.1 | 26.2 | 90.0 | 8 | 21.7 | 162.6 | - |
| IWR | 13.6 | 21.4 | 90.0 | 8 | 27.5 | 137.3 | R12 |
| ITH | 11.7 | 22.4 | 90.0 | 8 | 30.6 | 152.8 | R9 |
| ITR | 11.7 | 22.4 | 90.0 | 8 | 30.5 | 152.5 | R9 |

[a] Lamella parameters are lengths of two vectors defining the lamella plane and angle between them. [b] Per one side of the lamella. [c] The size of the channel is described using the ring (R) size, only T-atoms are counted.

### 3.2. Synthesis Feasibility Criteria of Zeolites

The theoretical number of possible zeolite frameworks is enormous.[21] But some of the zeolites can never be synthesized due to energetic and steric reasons. Unfortunately, there are no unambiguous rule to distinguish which zeolite can be synthesized and which is just hypothetical structure. Instead, we have to use various rules and treat the results with caution.

The stability of the zeolite is usually expressed as framework energy - computed energy per T-atom (average) relative to α-quartz reference. From this point of view the lower the framework energy is, the more stable the zeolite is. Often framework energy lower than 30 kJ/mol is considered as reasonable value for zeolite.[22] On the other hand tremendous number of hypothetical zeolites with low framework energy has not been prepared yet, proving that the energy is not the ultimate criterion.[35,22] It was shown, that for existing zeolites there is a correlation between framework energy and framework density (number of T-atoms per 1000 Å$^3$). With the least-square fit of this dependence we can confront our hypothetical zeolite structures – we can calculate the distance from the line,

$$\vartheta = |1.429 \times FD + FE - 39.914|/1.429. \qquad (12)$$

The distance $\vartheta$ is called a feasibility factor.[23] The lower the value of feasibility factor is, the more is the zeolite similar to "averaged" known zeolite.

We can also analyze geometric properties of the hypothetical material. Li *et al.* after statistical analysis of all existing zeolites proposed a set of rules,[24] which predicts the existence of hypothetic zeolites and thus their suitability for target synthesis. This set of rules is based on analysis of local interatomic distances (LIDs). As a first step to analyze LID criteria for a particular zeolite the structure of the zeolite must be optimized (as pure silica) using the SLC potential. Then for all bonds the T-O bond-lengths are computed. Moreover, for the bonded O-T-O and T-O-T groups of atoms the O-O and T-T distances were calculated. For all three sets (T-O, O-O and T-T) of local interatomic distances the mean value (denoted as $\langle D_{XX} \rangle$ ), the standard deviation (denoted $\sigma_{XX}$ ) and the difference between maximum and minimum distance (denoted $R_{XX}$ ) is computed.

**Table 2.** Overview of LID criteria

| Criterion number | Criterion | | |
|---|---|---|---|
| 1 | $\lvert\langle D_{OO}\rangle - 1.6284 \times \langle D_{TO}\rangle - 0.0071\rvert \leq 0.0009$ Å | | |
| 2 | $\lvert\langle D_{TT}\rangle + 4.8929 \times \langle D_{TO}\rangle - 10.9128\rvert \leq 0.0046$ Å | | |
| 3 | $\sigma_{TO} \leq 0.0196$ Å | $\sigma_{OO} \leq 0.0588$ Å | $\sigma_{TT} \leq 0.0889$ Å |
| 4 | $R_{TO} \leq 0.0634$ Å | $R_{OO} \leq 0.2746$ Å | $R_{TT} \leq 0.3332$ Å |
| 5 | $\langle D_{TO}\rangle \in \langle 1.5967; 1.6076\rangle$ Å | $\langle D_{OO}\rangle \in \langle 2.6070; 2.6251\rangle$ Å | $\langle D_{TT}\rangle \in \langle 3.0490; 3.0998\rangle$ Å |
| | $\langle D_{TO}\rangle \in \langle 1.5991; 1.6284\rangle$ Å | $\langle D_{OO}\rangle \in \langle 2.6111; 2.6588\rangle$ Å | $\langle D_{TT}\rangle \in \langle 2.9435; 3.0882\rangle$ Å |

The first two criterions reflect the average properties of the zeolite. The meaning of the first criterion is that with increasing T-O distance the O-O distance is also rising, leaving the tetrahedron without deformation (almost ideal tetrahedron shape). The second rule describes the connection between these tetrahedra. In contrast with the first two criterions, the third criterion is half way between average and local properties of the zeolite. The fourth has entirely local character and thus inform us about stretched bonds and local strain. The fifth criterion describes the LID parameters for conventional (1st row) and unconventional (2nd row; the criterion for unconventional zeolite was mentioned for comparison) zeolites. Notice that there is an overlap between these groups. According to Li, all the most used zeolites in industry are conventional zeolites, due to their higher stability. If the zeolite does not fulfill the criterion for conventional zeolite, it fails the fifth criterion.

There are more approaches to guess the zeolite feasibility, however, as was already told, none of them is absolutely reliable. Even if the LID criteria are satisfied by all existing zeolites, it just reflects the fact that they are parameterized that way and structure satisfying them does not have to be realizable and vice versa (that might lead to reparameterization of the criteria). To mention some of the other approaches, one of them is called flexibility window and describes the ability of zeolite exist in various range of framework densities without deformation of ideal $TO_4$ tetrahedron. This degree of freedom can be important during the zeolite synthesis.[36] The comparison of tetrahedra with ideal tetrahedron is often used for feasibility assessments.[37] Although we do not use all the methods for feasibility evaluation, many of them are reflected in the LID criteria.

### 3.3. Modeling of -D4R Materials

*3.3.1. Organization and Reassembly Process*

Forming of interlamellar hydrogen bonds is fundamental for organization phase of the ADOR process. During a calcination process a condensation reaction between silanol groups forming these hydrogen bonds occurs. When we modeled the organization and reassembly phase, instead of forming hydrogen bonds we tried to overlap silanol oxygen atoms – thus we reflected both the hydrogen bonds formation and condensation reaction. The modeling (without addition of silylation agent, leading thus to -D4R materials) was done as follows: The grid of all relative positions of the lamellae were prepared, which means the square grid from (0,0) to (1,1), where the numbers in brackets denote the relative shift in two directions (in fractional coordinates with respect to fundamental arrangement) defining the plane of the lamella. For every point of that grid the sum of squares of the shortest (uniquely assigned; it caused the cusps on the objective function) silanol oxygen-oxygen distances was calculated. By finding local minima of this objective function (which illustrates the forming of hydrogen bonds needed for condensation reaction) the favorable relative positions of the lamellae were chosen. Then the atoms relevant to condensation reaction were removed and the distance between lamellae and unit cell parameters were adjusted. This way the initial (or we can say starting) structures were obtained.

For the ITR case, where two lamellae are present in the unit cell, the procedure described above results in a set of new lamellae (formed by two connected former lamellae) and for every such lamella the procedure must be repeated to get fully-condensed initial guess structure.

For all the starting structures a topological analysis was performed. Using home-made MATLAB[38] code, the topologically unique structures were chosen by comparing their unique coordination sequences (CS) and vertex symbols (VS).*

* For every T-atom, the coordination sequence and vertex symbol can be evaluated. Coordination sequence counts how many "new" T-atoms we can "visit" in each step if we travel over T-O-T connections. The first number is always 4 for fully condensed zeolites, because $TO_4$ unit is connected to another 4 T-atoms. With higher number of steps, the number of "new" T-atoms rises dramatically, because of the spherical character of coordination sequences. The vertex symbol characterizes the smallest rings on all the six O-T-O angles in tetrahedron. Just T-atoms are counted for the ring size and its multiplicity is also considered. The pairs of opposing angles are grouped together.

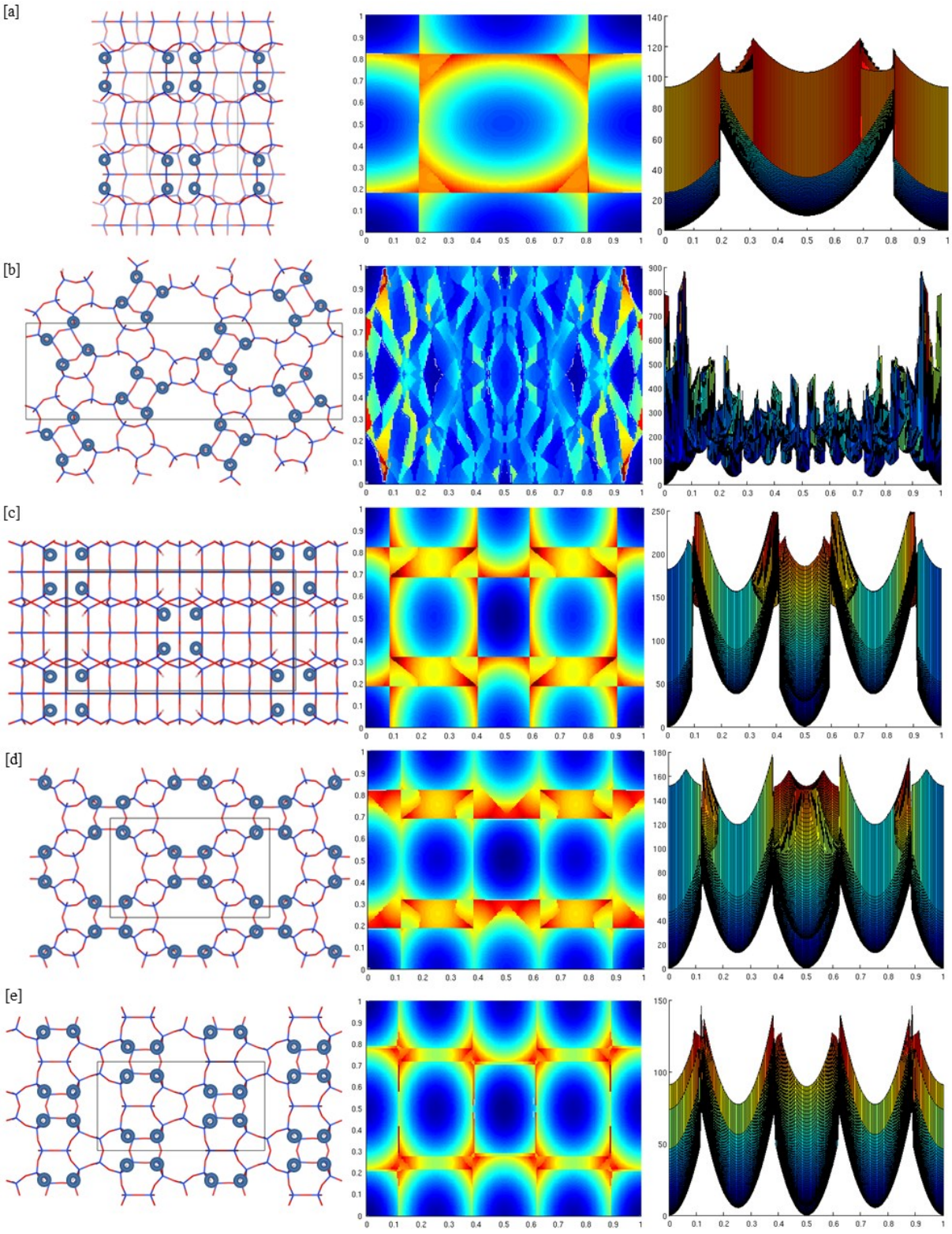


**Figure 3.** Lamella and objective function for [a] UTL, [b] IWW, [c] IWV, [d] IWR and [e] ITH parent zeolite. Both identical sides of ITR lamella are similar to ITH and thus it is not depicted here. Unit cell and silanol groups on upper side marked on the lamella (grey line and blue circles, respectively). From above and side view of the penalty function depicted for better illustration. Note that the fundamental arrangement (0,0) has always zero value of objective function. Number of silanol groups must be taken into account when comparing objective function values between materials formed from different lamellae.

In this work we assumed this way of comparing zeolites sufficient to distinguish between different zeolites, although situation where two different zeolites have the same unique CS/VS characteristics can occur rarely.[39] Also the CS/VS characteristics were compared with existing zeolites. The only match was for the PCR zeolite (reported as UTL-D4R(C2/m) structure), which had to be found due to our methodology. All other hypothetical zeolites had new topologies.

For the two-lamellar ITR-based materials 10 unique topologies were found, corresponding to only 4 topologically unique connections between the lamellae. Both sides of the forming lamellae are topologically identic, so for the PBE optimization were chosen just 4 structures having the 4 topologically unique connections on one side and the second connection was kept fixed and corresponded to the lamella arrangement in parent zeolite (fundamental arrangement – for definition see Figure 2). This way, we tested the energetic effect of different connections, however an assumption, that connection on one side of lamella didn't influence the connection on the other side, was necessary. In the case of IWW-based materials the number of hypothetical topologies was higher, however most of the topologies are not chemically reasonable. Just three unique structures with the lowest value of objective function were optimized using the PBE functional[28]. For other zeolite families – ITH-D4R, IWR-D4R, IWV-D4R and UTL-D4R – all topologically unique structures found (3, 3, 3 and 4, respectively) were optimized at the PBE level.

The topologically unique structures were optimized at the PBE level. To report structures with their symmetry a symmetrization using PLATON program[40] was used. Of course, the symmetrization changed the geometry – it might not reach the optimization criteria anymore, so the optimization and symmetrization was repeated and the changes in energy were monitored during the whole process (optimization-symmetrization-optimization-symmetrization; see Table A1 in Appendix A). Using this iterative way we confirmed, that the structures have the right symmetry and that they are also local minima (stationary point) on the potential energy surface, or at least they are as close to local minima as possible for the symmetrized structures. The notation used for reported structures is XYZ-D4R(SYM), where XYZ is the parent zeolite International Zeolite Association[1] framework type code, -D4R (or -S4R in the following section) is the relative difference of the linker with respect to the parent zeolite and SYM is the symmetry of the material. For two structures (ITH-D4R(Amm2) and IWR-D4R(Cmmm)) the final framework energy was about 1 kJ/mol higher than the energy before the first symmetrization, so the symmetry might be artificial and the structure without symmetry were also reported (as ITH-D4R($P1_{Amm2}$) and IWR-D4R($P1_{Cmmm}$)).

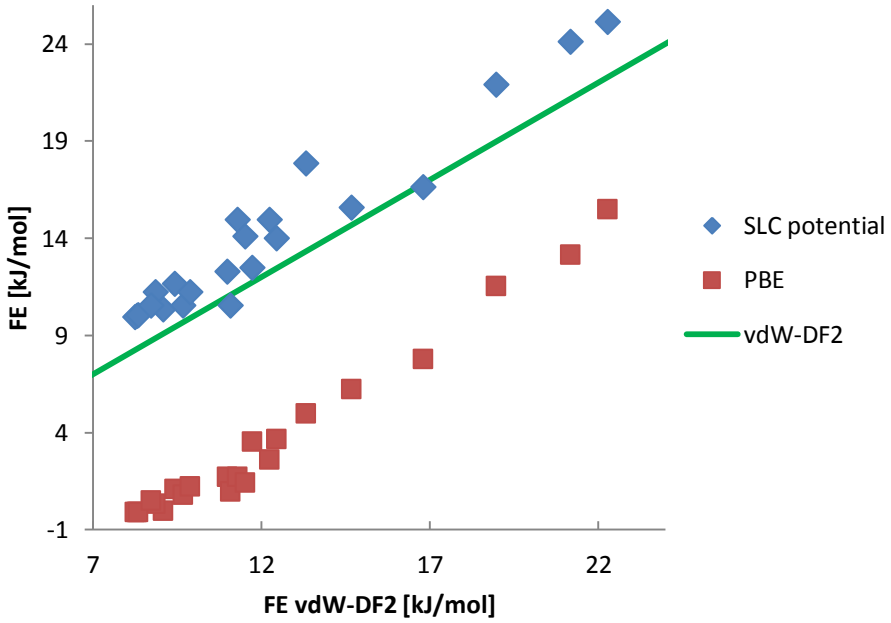


**Figure 4.** Comparison of SLC potential and PBE functional with vdW-DF2 reference

The framework energies obtained using PBE doesn't contain dispersion, so single-point calculation using the vdW-DF2 functional[29] was made to include dispersion effects. The vdW-DF2 energies are reported as DFT energies (i.e. $FE_{DFT}$). We assumed that PBE optimization is sufficient for these strongly covalently-bonded systems. The dispersion should have minimal effect on the geometry (probably lowers the cell volume slightly), because it can't compress a system with such structure of covalent bonds much. Moreover, use of the vdW-DF2 functional for optimization would increase the computational cost too much.

We also tried to optimize the starting structures using a force field. As will be discussed later, the SLC potential performed quite well (results reported as FF, i.e. $FE_{FF}$). All 10 topologically unique topologies were optimized for ITR-D4R materials. For the IWW-D4R materials we were able to optimize 5 unique topologies, but MATLAB[38] preoptimization code had to be used (discussed later in the -S4R section). As a result we have 2 more structures for IWW-D4R materials using force field in comparison with using DFT, however these two structures are quite high in energy. For ITH-, IWR- and UTL- based zeolites we also tested optimization of the final force field structures using PBE. In most cases the PBE energies for optimization from initial guess and from preoptimized (by force field) structure are similar, indicating to similar geometries. In two cases (ITH-D4R(Cm) and UTL-

D4R(Pm)) the PBE optimization starting from final force field structure gave noticeably lower energy than the one from initial guess, which corresponded to situation where different local minimum was found. For the UTL case the energy difference did not mean any qualitative change, on the other hand, for the ITH case the optimization from initial guess predicted the ITH-D4R(Cm) as the only ITH-based energetically disfavored structure, in contrast with the optimization from force field preoptimized structure, which predicted the structure energetically comparable to other. To avoid the false impression, that one ITH-based structure is disfavored, we reported the results for structure preoptimized by force field (with the consistent methodology used).

### *3.3.2. Hypothetical -D4R Zeolites*

The resulting energies of SLC potential, PBE functional and vdW-DF2 are compared in Figure 4. It should be pointed out, that there is a correlation between objective function and energy (see Table A3 in Appendix A), however small differences in objective function are not reliable for comparison of stability (energy). Using the vdW-DF2 data as a reference, the other methods are quite consistent (with respect to the fact, that PBE does not contain dispersion contribution), but the force field energies fluctuates more. The PBE data systematically underestimates the framework energy. This negative shift is caused by the missing dispersion contribution, which is similar for all systems, as they have quite similar framework density. This way we validate the reliability of SLC potential for further use in the -S4R section. We estimated that the use of force field preoptimization can save about 20 % of computational cost, although in some particular cases the force field preoptimization increase the cost. This corresponds to cases where the force field artificially lowers the symmetry, which is than restored by DFT optimization during high number of optimization steps.

The results are summarized in Table 3. There is a significant difference between UTL-D4R, IWW-D4R, IWV-D4R and IWR-D4R, ITH-D4R, ITR-D4R data. For the former three families of materials there is one strongly energetically preferred structure (corresponding to fundamental arrangement). For the other there are only small energetic differences, in some cases all the structures are almost isoenergetic. For an interpretation of this fact, let's take a look at the forming lamella properties. By the D4R removal a quartet of silanols is formed, these four silanol groups are relatively close together and we can call them "silanol hills". If the distance between these silanol hills on lamella is large, then the preferred way of forming interlamellar connections is simple condensation reaction between two silanol hills on adjacent lamellae (one silanol hill on every lamella). Other ways of forming interlamellar

connections (condensation between one silanol hill on one lamella and more than one silanol hills on the other lamella) may need lamella deformation to bring the silanol hills closer and thus the energy is increased dramatically.

For the UTL- and IWV-based lamellae, the silanol hills are far from others. This fact is reflected even in the lowest silanol density values from studied lamellae (see Table 1). For the IWW case the explanation is different, the silanol quartets are turned diversely on the lamella and thus the geometry constraints for connections are strict. All 3 IWW-D4R structures optimized by PBE have the silanol hills condensed in the "1 with 1" way, but just one have the silanols turned in the same way and lead thus to significantly lower energy. The 2 extra structures optimized just by force field have the silanol hills condensed in the "1 with more" way and both are high in energy, with respect to the lowest-energy structure. In contrast, the ITH and ITR lamellae have the highest silanol density and the silanols form a rectangular grid with almost ideal distance between silanols. This arrangement explains the small energy differences, because various connections are possible without stretching bonds and lamella deformation. IWR case is similar, although the arrangement is not as ideal as in the ITH/ITR case.

The structures with the same lamella arrangement as the parent zeolite has (fundamental arrangement) are always energetically favored or at least they have low energy in comparison to structures with relative shift between lamellae (all the first materials for every parent zeolite in the Table 3 are the non-shifted structures). This reflects the fact that the both sides of lamellae are topologically identical, having thus the silanol groups placed symmetrically (in positions of former D4R units) leading to formation of strong hydrogen bonds without lamella deformation in the fundamental arrangement. In a group of related materials (e.g. UTL-D4R family) the structures with higher framework density have often higher energy. This is a consequence of stretched linkers, which can bring the lamellae closer. The framework density is related to lamella dimensions (the former lamella can still be recognized in the zeolite) and interlamellar separation. From the results it is obvious that the -D4R zeolites have longer lamella dimensions than the parent zeolites (except the strained structures, where the lengths can be even shorter). The lamella size is probably dependent on the connections – the more strained connection the shorter lamella lengths (the lamella matter is pulled by the linkers, leading to deformation and shorter lamella cell lengths). The LID criteria (for definition see section 3.2) are always satisfied for the lowest-energy structure. That means that the zeolite should be stable and thus suitable for target synthesis. For the ITH-D4R and ITR-D4R all modeled systems fulfill these criteria. However, the energy values

**Table 3.** Characteristics of -D4R materials and their comparison to parent zeolites

| Zeolite | $FE_{DFT}$[a] | $FE_{FF}$[a] | $FD_{DFT}$[a] | $FD_{FF}$[a] | Lamella parameters[b] | | | Feasibility factor $\vartheta$[a] | LID criteria[a] | | | | |
|---|---|---|---|---|---|---|---|---|---|---|---|---|---|
| | [kJ/mol] | [kJ/mol] | [$10^{-3}$Å$^{-3}$] | [$10^{-3}$Å$^{-3}$] | [Å] | [Å] | [deg] | | 1 | 2 | 3 | 4 | 5 |
| UTL | 12.0 | 15.3 | 15.1 | 15.8 | 12.5 | 14.1 | 90.0 | | | | | | |
| -D4R(C2/m) | 9.1 | 10.4 | 18.1 | 19.3 | 12.6 | 14.2 | 90.0 | 1.4 | 1 | 1 | 1 | 1 | 1 |
| -D4R(Pm) | 11.7 | 12.5 | 19.0 | 20.2 | 12.6 | 14.0 | 90.0 | 1.0 | 1 | 1 | 1 | 1 | 1 |
| -D4R(P1) | 12.5 | 14.0 | 18.7 | 19.8 | 12.2 | 14.2 | 89.7 | 1.7 | 0 | 1 | 1 | 0 | 1 |
| -D4R(Pm') | 14.7 | 15.6 | 19.3 | 20.6 | 12.2 | 13.9 | 90.0 | 3.5 | 0 | 1 | 0 | 0 | 1 |
| IWW | 11.7 | 13.8 | 15.9 | 16.8 | 13.1 | 42.5 | 90.0 | | | | | | |
| -D4R(Pbam) | 11.0 | 12.3 | 17.9 | 19.1 | 13.3 | 42.7 | 90.0 | 0.2 | 1 | 1 | 1 | 1 | 1 |
| -D4R(C2/c) | 19.0 | 21.9 | 19.9 | 21.0 | 12.6 | 42.6 | 90.0 | 8.4 | 0 | 1 | 0 | 0 | 0 |
| -D4R(Aba2) | 22.3 | 25.1 | 20.7 | 21.8 | 12.3 | 42.9 | 90.0 | 11.4 | 0 | 1 | 0 | 0 | 0 |
| IWV | 13.3 | 14.6 | 14.7 | 15.8 | 14.1 | 26.2 | 90.0 | | | | | | |
| -D4R(Fmmm) | 11.1 | 10.6 | 18.0 | 19.9 | 14.1 | 26.0 | 90.0 | 0.7 | 1 | 1 | 1 | 1 | 1 |
| -D4R(Cmm2) | 16.8 | 16.6 | 18.9 | 20.6 | 13.8 | 25.5 | 90.0 | 4.3 | 0 | 1 | 0 | 0 | 1 |
| -D4R(C2/m) | 21.2 | 24.1 | 20.2 | 21.6 | 13.7 | 25.7 | 90.0 | 10.5 | 0 | 1 | 0 | 0 | 0 |
| IWR | 12.1 | 15.5 | 15.2 | 15.9 | 13.6 | 21.4 | 90.0 | | | | | | |
| -D4R($P1_{Cmmm}$) | 11.3 | 15.0 | 17.1 | 18.0 | 13.7 | 21.7 | 90.0 | 0.5 | 1 | 1 | 1 | 1 | 1 |
| -D4R(C2/m) | 11.5 | 14.1 | 17.8 | 18.8 | 13.6 | 21.8 | 90.0 | 0.7 | 1 | 1 | 1 | 1 | 1 |
| -D4R(Cmmm) | 12.3 | 15.0 | 17.1 | 18.0 | 13.7 | 21.7 | 90.0 | 0.5 | 1 | 1 | 1 | 1 | 1 |
| -D4R(Fmmm) | 13.3 | 17.8 | 18.0 | 18.9 | 13.7 | 21.7 | 90.0 | 3.5 | 1 | 1 | 1 | 1 | 0 |
| ITH | 10.4 | 12.4 | 16.8 | 17.8 | 11.7 | 22.4 | 90.0 | | | | | | |
| -D4R($P1_{Amm2}$) | 8.9 | 11.2 | 19.1 | 20.4 | 11.8 | 22.6 | 90.0 | 0.3 | 1 | 1 | 1 | 1 | 1 |
| -D4R(Cm) | 9.4 | 11.7 | 19.4 | 20.6 | 11.9 | 22.5 | 90.0 | 0.9 | 1 | 1 | 1 | 1 | 1 |
| -D4R(Cm') | 9.7 | 10.5 | 19.3 | 20.6 | 11.9 | 22.4 | 90.0 | 0.1 | 1 | 1 | 1 | 1 | 1 |
| -D4R(Amm2) | 9.9 | 11.2 | 19.0 | 20.4 | 11.8 | 22.7 | 90.0 | 0.3 | 1 | 1 | 1 | 1 | 1 |
| ITR | 10.4 | 12.5 | 16.8 | 17.7 | 11.7 | 22.4 | 90.0 | | | | | | |
| -D4R(P21/m) | 8.3 | 10.0 | 19.3 | 20.5 | 11.8 | 22.5 | 89.9 | 0.4 | 1 | 1 | 1 | 1 | 1 |
| -D4R(P-1) | 8.3 | 10.0 | 19.4 | 20.8 | 11.8 | 22.4 | 89.9 | 0.2 | 1 | 1 | 1 | 1 | 1 |
| -D4R(C2/m) | 8.4 | 10.1 | 19.4 | 20.7 | 11.8 | 22.4 | 90.0 | 0.2 | 1 | 1 | 1 | 1 | 1 |
| -D4R(C2/m') | 8.7 | 10.6 | 19.4 | 20.8 | 11.9 | 22.4 | 90.0 | 0.2 | 1 | 1 | 1 | 1 | 1 |

[a] For definition see section 3.2. [b] Lamella parameters are lengths of two vectors defining the lamella plane and angle between them.

are similar and thus can be difficult to synthesize regular zeolite and not an irregular product. It would be an object of further research, whether use of appropriate SDA can lead the synthesis to regular product (for the fundamental arrangement this problem might be irrelevant, because the hydrolysis of parent zeolite should lead to lamellae having the fundamental arrangement). These problems are not present in the cases of UTL-D4R, IWW-D4R and IWV-D4R, where the energetically preferred structure is predicted. However, for the synthesis of structures with higher energy, it will be necessary to estimate the extent of SDA effect. At this moment we do not know, how large energetic difference can be overcome by the use of SDA.

### 3.4. Modeling of -S4R Materials

#### *3.4.1. Organization and Reassembly Process*

The modeling of the organization phase with the addition of silylation agent was done in a different way with respect to -D4R materials. As was already told, only formation of S4R unit is considered, leading thus to materials, where the lamellae are connected by S4R linkers instead of D4Rs. The resulting materials are denoted as -S4R materials.

Firstly, the positions on the lamellae, where the S4R can be placed, were analyzed – for every possible quartet of silanols the distances between oxygen atoms were computed and evaluated whether they are reasonable for binding a S4R unit. Secondly, all simultaneously occurring S4R positions were analyzed (this reflects the obvious fact that every silanol may be connected to only one S4R, so some combinations of possible S4Rs cannot exist at the same time). With the S4R positions specified on both sides of the lamella/lamellae, we tried to "overlap" them using lamella translation and thus we modeled the effect of relative positions of the lamellae (two overlapped S4R units correspond to one S4R in the final material). For every point of the translation grid the sum of squares of S4R-S4R distances (more precisely, the distance between S4R geometric centers) were evaluated. By finding local minima of this function, the optimal structures with reasonable S4R positions were found. This was done for all combinations of simultaneously occurring S4Rs on both relevant sides of lamellae. Structures which have any S4R-S4R distance longer than 2 Å were considered as non-stable or too strained and were not modeled. Thereafter the S4Rs were added in the structures physically. In that point the S4Rs were added as a rigid object, however rotation was used to minimize the interatomic distances in the least square sense. The objective function was calculated as sum of squares of the shortest silanol oxygen – S4R silicon distances (treated

just in 2 dimensions, because the silanol oxygens always lie in an almost ideal plane and distance in perpendicular direction is thus irrelevant). This is in fact second objective function used for the -S4R materials modeling as the first described the distances between S4Rs. However, the first objective function was used just for prescreening, this second objective function based on Si-O distances is much more informative and is therefore used as a characteristics of the structure (in Appendix A – Table A4). Notice that the objective function in -D4R section is different and thus not directly comparable. For the -S4R materials the Si-O distances were computed (not O-O) and the S4R has connections on both sides leading to twice the number of contribution terms with respect to the -D4R objective function.

Unfortunately, the structures made this way often had very stretched bonds, so for the structures with S4Rs added a simple preoptimalization was performed. The code used to preoptimalization recognized all the bonds and then in an iterative manner tried to shorten the Si-O bonds exceeding 1.8 Å (without changing the unit cell parameters). Thanks to the iterative character of the code, the too stretched bonds were partially relaxed without breaking other bonds.

As the reliability of the force field was confirmed in the previous section, we used force field optimization as a preoptimization for DFT calculations. This was necessary, because the number of topologically unique structures was much higher for -S4R materials than for the -D4R materials and the force field energies were needed as a prescreening. The high number of topologies was due to the S4R linkers (which can be placed in different positions) together with relative arrangement of the lamellae.

The topological analysis was performed. The structures referred as UTL-S4R(C2) and IWV-S4R(P1) correspond to known zeolites with OKO and NES topology, respectively. For all topologically unique structures we tried to optimize the structures by force field. However, some too stretched structures we were not able to optimize (some IWR-S4R, IWV-S4R and IWW-S4R materials). In one case the force field led to collapse of the structure, because some silicon and oxygen atoms got too close during the optimization and the Coulombic term moved them even closer, leading to unphysical structure with more than four bonds on silicon. This failure was a consequence of the force field formulas, where no bonds and tetrahedral constraints for silicon atoms were considered. We were able to optimize this structure from different, topologically equivalent structure. It should be pointed out that this was the only case where the force field completely failed, in other situations it performed quite well (except artificially lowered the symmetry). Just to be sure that the final structure was reasonable some simple topologic tests were used – tetrahedrally coordinated silicon

atoms and no change of topology during optimization tested (these tests were applied even for the -D4R structures).

The structures with lowest force field energy† were afterwards optimized using PBE functional (starting from force field optimized structure) in the same way as in the -D4R section (optimization-symmetrization-optimization-symmetrization, see Table A2) and single-point calculation using the vdW-DF2 functional was performed. This time, more possible symmetries were found by the PLATON software package[40] in some cases. We reported the structures with higher symmetry, because no significant difference in energy with respect to higher symmetry was observed.

### *3.4.2. Hypothetical -S4R Materials*

The results for -S4R materials (Table 4, appendix Table A4) shows some similar features as for -D4R materials. Again, higher strain leads to lower framework density and for the UTL-S4R, IWW-S4R and IWV-S4R materials there is one energetically preferred structure corresponding to fundamental arrangement (with S4R placed in the positions of the original D4R). For the UTL-S4R and IWV-S4R cases the preference is even higher than for the -D4R materials (from 2.6 kJ/mol to 7.6 kJ/mol for the UTL case). It is caused by the structural constraint of S4R – just some positions on the lamellae are able to bind this linker (without energetic penalty) and the position where the D4R in the parent zeolite was located must be able to bind the similar S4R unit. In contrast to -D4R materials, the IWR-S4R materials have one preferred structure – the explanation of this fact is the same as for UTL-S4R and IWV-S4R preferred structures – the S4R structural constraint. For the IWW-S4R the preference of the structure is lower than in the -D4R case (from 8 kJ/mol decreased to only 4.5 kJ/mol), this atypical behavior reflects the ability of S4R compensate turned silanol quartets. For the ITH-S4R and ITR-S4R zeolites no preferred structure is observed for the same reason as for the

-D4R materials. The framework energies of -S4R materials are higher and framework densities lower than for -D4R analogues. On the contrary, the IWV-S4R(P1) structure (known zeolite with NES framework type) has lower DFT framework energy than IWV-D4R(Fmmm) analogue. It can be effect of too high symmetry of the reported IWV-D4R(Fmmm) structure,

† To keep the computational cost bearable, we optimized this way all ITH-S4R zeolites satisfying LID criteria and all ITR-S4R structures to 1 kJ/mol with respect to lowest energy structure. For the IWV-S4R case only one zeolite was optimized using DFT, because the other structures have about 8.8 kJ/mol (and more) higher framework energy, which seems to be too much for a feasible synthesis. Moreover the distance between silanol groups is too large and formation of S4R is thus questionable.

**Table 4.** Characteristics of -S4R materials and their comparison to parent zeolites

| Zeolite | $FE_{DFT}$[a] | $FE_{FF}$[a] | $FD_{DFT}$[a] | $FD_{FF}$[a] | Lamella parameters[b] | | | Feasibility factor $\vartheta$[a] | LID criteria[a] | | | | |
|---|---|---|---|---|---|---|---|---|---|---|---|---|---|
| | [kJ/mol] | [kJ/mol] | [$10^{-3}$Å$^{-3}$] | [$10^{-3}$Å$^{-3}$] | [Å] | [Å] | [deg] | | 1 | 2 | 3 | 4 | 5 |
| UTL | 12.0 | 15.3 | 15.1 | 15.8 | 12.5 | 14.1 | 90.0 | | | | | | |
| -S4R(C2) | 11.2 | 13.8 | 17.0 | 17.8 | 12.6 | 14.0 | 90.0 | 0.5 | 1 | 1 | 1 | 1 | 1 |
| -S4R(P1) | 18.8 | 22.2 | 18.0 | 18.9 | 12.1 | 13.9 | 89.7 | 6.5 | 0 | 1 | 0 | 0 | 1 |
| -S4R(Pm) | 18.8 | 23.3 | 18.5 | 19.3 | 12.6 | 13.4 | 90.0 | 7.7 | 0 | 1 | 0 | 0 | 1 |
| -S4R(P1') | 21.0 | 24.1 | 18.8 | 19.7 | 11.8 | 13.8 | 89.8 | 8.7 | 0 | 1 | 0 | 0 | 1 |
| IWW | 11.7 | 13.8 | 15.9 | 16.8 | 13.1 | 42.5 | 90.0 | | | | | | |
| -S4R(P1) | 11.6 | 13.5 | 18.2 | 19.1 | 12.7 | 41.6 | 90.0 | 0.6 | 1 | 1 | 1 | 1 | 1 |
| -S4R(C2/c) | 16.1 | 19.2 | 18.5 | 19.3 | 12.7 | 41.3 | 90.0 | 4.8 | 0 | 1 | 0 | 0 | 1 |
| IWV | 13.3 | 14.6 | 14.7 | 15.8 | 14.1 | 26.2 | 90.0 | | | | | | |
| -S4R(P1) | 10.3 | 12.5 | 16.9 | 17.8 | 13.9 | 25.6 | 89.9 | 1.4 | 1 | 1 | 1 | 1 | 1 |
| IWR | 12.1 | 15.5 | 15.2 | 15.9 | 13.6 | 21.4 | 90.0 | | | | | | |
| -S4R(C2/m) | 12.3 | 16.2 | 17.4 | 18.0 | 13.5 | 20.4 | 90.0 | 1.4 | 1 | 1 | 1 | 1 | 1 |
| -S4R(Cmcm) | 14.8 | 18.4 | 18.5 | 19.6 | 13.0 | 21.0 | 90.0 | 4.6 | 1 | 1 | 1 | 0 | 0 |
| -S4R(Immm) | 17.1 | 21.1 | 18.3 | 19.3 | 13.1 | 21.0 | 90.0 | 6.2 | 1 | 1 | 1 | 1 | 0 |
| ITH | 10.4 | 12.4 | 16.8 | 17.8 | 11.7 | 22.4 | 90.0 | | | | | | |
| -S4R(Cmc21) | 9.3 | 11.2 | 18.7 | 19.8 | 11.5 | 22.2 | 90.0 | 0.3 | 1 | 1 | 1 | 1 | 1 |
| -S4R(Cm) | 9.4 | 11.4 | 18.7 | 19.7 | 11.5 | 22.3 | 90.0 | 0.2 | 1 | 1 | 1 | 1 | 1 |
| -S4R(P1) | 9.5 | 11.1 | 19.2 | 20.2 | 11.4 | 22.0 | 89.9 | 0.0 | 1 | 1 | 1 | 1 | 1 |
| -S4R(Cm') | 9.6 | 12.0 | 18.7 | 19.7 | 11.5 | 22.2 | 90.0 | 0.2 | 1 | 1 | 1 | 1 | 1 |
| -S4R(Imm2) | 10.3 | 12.4 | 18.6 | 19.7 | 11.6 | 22.0 | 90.0 | 0.4 | 1 | 1 | 1 | 1 | 1 |
| -S4R(Cm'') | 10.7 | 13.6 | 18.9 | 19.8 | 11.5 | 22.1 | 90.0 | 1.4 | 1 | 1 | 1 | 1 | 1 |
| -S4R(Cm''') | 11.3 | 14.0 | 18.8 | 19.8 | 11.6 | 22.1 | 90.0 | 1.6 | 1 | 1 | 1 | 1 | 1 |
| -S4R(Cm'''') | 12.3 | 14.7 | 19.1 | 20.1 | 11.3 | 22.5 | 90.0 | 2.4 | 1 | 1 | 1 | 1 | 1 |
| ITR | 10.4 | 12.5 | 16.8 | 17.7 | 11.7 | 22.4 | 90.0 | | | | | | |
| -S4R(Pnnm) | 9.3 | 11.3 | 18.8 | 19.8 | 11.5 | 22.1 | 90.0 | 0.2 | 1 | 1 | 1 | 1 | 1 |
| -S4R(C2/c) | 9.3 | 10.7 | 19.1 | 20.2 | 11.4 | 22.1 | 90.0 | 0.2 | 1 | 1 | 1 | 1 | 1 |
| -S4R(C2) | 9.4 | 11.3 | 18.8 | 19.9 | 11.4 | 22.1 | 90.0 | 0.1 | 1 | 1 | 1 | 1 | 1 |
| -S4R(P-1) | 9.5 | 11.3 | 18.9 | 19.9 | 11.5 | 22.0 | 89.9 | 0.1 | 1 | 1 | 1 | 1 | 1 |
| -S4R(Cm) | 9.5 | 11.4 | 18.8 | 19.9 | 11.4 | 22.2 | 90.0 | 0.1 | 1 | 1 | 1 | 1 | 1 |
| -S4R(P1) | 9.5 | 11.6 | 18.9 | 19.8 | 11.5 | 22.1 | 90.0 | 0.1 | 1 | 1 | 1 | 1 | 1 |
| -S4R(P21) | 9.7 | 11.6 | 18.7 | 19.7 | 11.5 | 22.3 | 89.9 | 0.1 | 1 | 1 | 1 | 1 | 1 |
| -S4R(P-1') | 9.7 | 11.6 | 18.7 | 19.8 | 11.5 | 22.2 | 90.0 | 0.0 | 1 | 1 | 1 | 1 | 1 |
| -S4R(P-1'') | 9.7 | 11.6 | 18.9 | 20.0 | 11.5 | 22.0 | 90.0 | 0.1 | 1 | 1 | 1 | 1 | 1 |

[a] For definition see section 3.2. [b] Lamella parameters are lengths of two vectors defining the lamella plane and angle between them.

the force field energies[‡] support this hypothesis as the IWV-D4R(Fmmm) has lower energy than IWV-S4R(P1) according to force field.

The lamella dimensions are usually shorter than for parent zeolites and -D4R materials. This probably corresponds to more strained connections. Indeed, the S4R linker introduces higher strain than D4R unit (per T-atom, however D4R unit has twice the number of T-atoms). Non-ideal S4R position results in distortion of S4R $TO_4$ tetrahedra. Even the values of O-Si-O angles about 101 ° were observed. In contrast, the D4R unit can compensate the strain by bending the softer Si-O-Si angles, keeping the almost ideal tetrahedra with O-Si-O angles close to 109.5 °. The behavior of zeolites as ideal $TO_4$ tetrahedra with softer Si-O-Si connections is well-known and is used in many approximate modeling methods as well as for feasibility assessment.[37,36]

It seems that the IWR lamella shows the highest flexibility. This lamella is formed in some positions just by one layer of T-atoms and has the lowest T-atom density (137.3 T-atoms per 1000 $Å^2$), so this behavior is not much surprising.

Now it is time to discuss the feasibility of zeolite synthesis. It will be discussed together for -D4R and -S4R materials. Many of the predicted structures fulfill all the LID criteria. It should be pointed out that all the materials not satisfying the fifth LID criterion for conventional zeolite (LID 5 has 0 value) satisfies this criterion for unconventional zeolite. The framework energy of the modeled systems is often reasonable with respect to zeolite materials. The framework energies and framework densities for materials in Tables 3 and 4 were compared with linear fit for the known zeolites (see Figure 5). The feasibility factor of many modeled systems is smaller than 2.0, which is the highest value observed for parent zeolite used in this work (IWV). The lowest energy structure for every group (i.e. UTL-D4R) of materials seems to have feasible synthesis. Some other structures are also suitable for target synthesis. For the ITH- and ITR-based materials there are many promising topologies.

The lamella parameters in Table 3 and 4 can have another interesting application. They can be used for prediction of possible mixed materials and intergrowths, because the zeolites having similar lamella size can be connected together. Different lamella size should result in strained structure, because of the periodic character and silanol positions (but small differences can be compensated by lamella flexibility). The structure of final zeolite may

[‡] Force field structures were verified to be minima on potential energy surface, the DFT optimization can end in every stationary point.

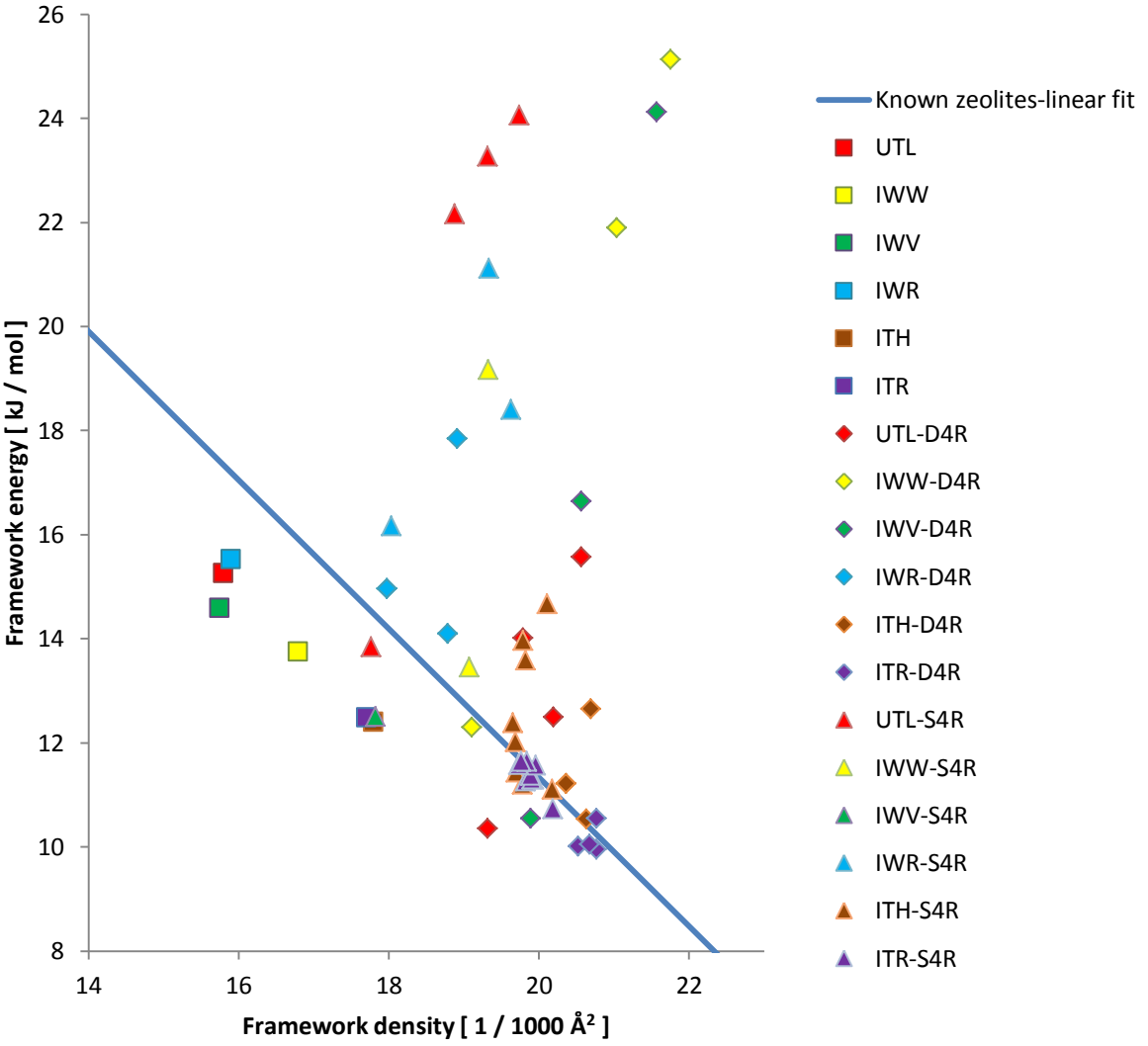


**Figure 5.** Feasibility expressed using framework energy – framework density dependence. Least square fit for known zeolites taken from article of Majda et al.[23] The SLC potential data are plotted here, the fit for vdW-DF2 data is not available, however it should show similar dependence.

be influenced even by the composition of reaction mixture (e.g. amount of silylation agent) and reaction conditions. Lately, new IPC-6 material was synthesized.[41] This material has alternating oxygen and S4R linkers. The class of materials based on UTL parent zeolite with alternating linkers was modeled (only fundamental arrangement and S4R in position of parent zeolite's D4R considered) and the results are shown in Table 5. These systems were modeled with two lamellae in the unit cell and thus the results can be slightly different from those shown in Table 3 and 4. The force field optimized structures were used as a starting structure for PBE optimization. The energy difference when going from D4R to S4R linker is significantly smaller than when going from S4R linker to oxygen linker. This reflects the fact that the structural constraint of S4R and D4R linker is similar and prevents the lamella

**Table 5.** Class of two-lamellar UTL-based zeolites with various linkers (linkers are described in parentheses with respect to parent zeolite – i.e. UTL(parent/-D4R) is a zeolite with D4R and oxygen linkers).

| Zeolite | $FE_{DFT}$[a] | $FE_{FF}$[a] | $FD_{DFT}$[a] | $FD_{FF}$[a] | Lamella parameters[b] | | |
|---|---|---|---|---|---|---|---|
| | [kJ/mol] | [kJ/mol] | [$10^{-3}$Å$^{-3}$] | [$10^{-3}$Å$^{-3}$] | [Å] | [Å] | [deg] |
| UTL(parent) | 12.0 | 15.3 | 15.0 | 15.8 | 12.5 | 14.1 | 90.0 |
| UTL(parent/-S4R) | 11.7 | 14.6 | 15.9 | 16.7 | 12.5 | 14.0 | 90.0 |
| UTL(parent/-D4R) | 10.6 | 13.1 | 16.3 | 17.2 | 12.6 | 14.1 | 90.0 |
| UTL(parent/-S4R-S4R) | 11.2 | 13.8 | 17.0 | 17.8 | 12.6 | 14.0 | 90.0 |
| UTL(parent/-S4R-D4R) | 10.4 | 12.5 | 17.5 | 18.5 | 12.5 | 14.1 | 90.0 |
| UTL(parent/-D4R-D4R) | 8.8 | 10.0 | 18.3 | 19.5 | 12.5 | 14.1 | 90.0 |

[a] For definition see section 3.2. [b] Lamella parameters are lengths of two vectors defining the lamella plane and a vector between them

relaxation. It seems that all these materials may be accessible, if the appropriate synthesis will be found.

For the zeolites modeled using DFT, the powder diffraction patterns were generated using the Mercury program.[42] This powder diffraction patterns may serve as a reference for synthesized materials identification.

# 4. Conclusion

The ADOR process or synthesis of new zeolites from lamellar precursors generally have potential to become widely used systematic way to synthesize new materials with tailored properties for industrial applications. We modeled the hypothetical products of the ADOR process using the Sanders-Leslie-Catlow force field and accurate DFT approach. Some of the modeled zeolites were found to be promising materials for target synthesis. Their synthesis feasibility was verified using various approaches: framework energy criterion, feasibility factor and LID criteria. The following conclusions can be drawn:

- For the UTL-, IWW- and IWV-based zeolites there is always one energetically preferred structure for every linker. Such structures should be accessible by the ADOR synthesis.
- For the IWR-based zeolites one preferred structure for the S4R linker was found, while several zeolite structures with similar energy were identified among IWR-D4R materials.
- For the ITH- and ITR-based materials there are many energetically favorable structures, and therefore the use of appropriate SDA may be needed.

Further investigation of the ADOR process mechanism is necessary to determine the role of SDA and other factors. Development of a reliable model for organization and reassembly phases would help us to find appropriate synthesis conditions. Modeling of the organization phase is a very demanding task, however, because lamellae, water molecules and SDA must be taken into account simultaneously.

The synthesis of parent zeolites with appropriate Si/Ge ratio is fundamental for successful application of the ADOR process and it represents another challenge for chemists. However, many more materials suitable for the ADOR process may be synthesized in the near future and the recently prepared ITG zeolite[43] is a clear indication of that.

# 5. References


1. Baerlocher, C.; McCusker, L. B. Database of Zeolite Structures. http://www.iza-structure.org/databases/.
2. Tschernich, R. W., In *Zeolites of the World*, Geoscience Press, Inc: Phoenix, Arizona, USA, 1992; pp 10-26.
3. Shamzhy, M. V.; Shvets, O. V.; Opanasenko, M. V.; Yaremov, P. S.; Sarkisyan, L. G.; Chlubna, P.; Zukal, A.; Marthala, V. R.; Hartmann, M.; Cejka, J., Synthesis of isomorphously substituted extra-large pore UTL zeolites. *J. Mater. Chem.* **2012,** *22* (31), 15793-15803.
4. Valtchev, V.; Majano, G.; Mintova, S.; Perez-Ramirez, J., Tailored crystalline microporous materials by post-synthesis modification. *Chem. Soc. Rev.* **2013,** *42* (1), 263-290.
5. Cundy, C. S.; Cox, P. A., The hydrothermal synthesis of zeolites: History and development from the earliest days to the present time. *Chem. Rev.* **2003,** *103* (3), 663-701.
6. Martinez, C.; Corma, A., Inorganic molecular sieves: Preparation, modification and industrial application in catalytic processes. *Coord. Chem. Rev.* **2011,** *255* (13-14), 1558-1580.
7. Pinar, A. B.; Marquez-Alvarez, C.; Grande-Casas, M.; Perez-Pariente, J., Template-controlled acidity and catalytic activity of ferrierite crystals. *J. Catal.* **2009,** *263* (2), 258-265.
8. Roth, W. J.; Cejka, J., Two-dimensional zeolites: dream or reality? *Catal. Sci. Technol.* **2011,** *1* (1), 43-53.
9. Roth, W. J.; Nachtigall, P.; Morris, R. E.; Čejka, J., Two-Dimensional Zeolites: Current Status and Perspectives. *Chem. Rev.*, DOI: 10.1021/cr400600f
10. Smith, R. L.; Eliášová, P.; Mazur, M.; Attfield, M. P.; Čejka, J.; Anderson, M. W., Atomic Force Microscopy of Novel Zeolitic Materials Prepared by Top-Down Synthesis and ADOR Mechanism. *Chem-Eur. J.*, *in press*
11. Roth, W. J.; Nachtigall, P.; Morris, R. E.; Wheatley, P. S.; Seymour, V. R.; Ashbrook, S. E.; Chlubna, P.; Grajciar, L.; Polozij, M.; Zukal, A.; Shvets, O.; Cejka, J., A family of zeolites with controlled pore size prepared using a top-down method. *Nat. Chem.* **2013,** *5* (7), 628-633.
12. Momma, K.; Izumi, F., VESTA: a three-dimensional visualization system for electronic and structural analysis. *J. Appl. Crystallogr.* **2008,** *41*, 653-658.
13. Schaack, B. B.; Schrader, W.; Schuth, F., How are Heteroelements (Ga and Ge) Incorporated in Silicate Oligomers? *Chem.-Eur. J.* **2009,** *15* (24), 5920-5925.
14. Corma, A.; Diaz-Cabanas, M. J.; Jiang, J.; Afeworki, M.; Dorset, D. L.; Soled, S. L.; Strohmaier, K. G., Extra-large pore zeolite (ITQ-40) with the lowest framework density containing double four- and double three-rings. *Proc. Natl. Acad. Sci. U. S. A.* **2010,** *107* (32), 13997-14002.
15. Sastre, G.; Vidal-Moya, J. A.; Blasco, T.; Rius, J.; Jorda, J. L.; Navarro, M. T.; Rey, F.; Corma, A., Preferential location of Ge atoms in polymorph C of beta zeolite (ITQ-17) and their structure-directing effect: A computational, XRD, and NMR spectroscopic study. *Angew. Chem.-Int. Edit.* **2002,** *41* (24), 4722-4726.

16. Corma, A.; Navarro, M. T.; Rey, F.; Rius, J.; Valencia, S., Pure polymorph C of zeolite beta synthesized by using framework isomorphous substitution as a structure-directing mechanism. *Angew. Chem.-Int. Edit.* **2001,** *40* (12), 2277-+.
17. Roth, W. J.; Dorset, D. L., The role of symmetry in building up zeolite frameworks from layered zeolite precursors having ferrierite and CAS layers. *Struct. Chem.* **2010,** *21* (2), 385-390.
18. Zhao, Z. C.; Zhang, W. P.; Ren, P. J.; Han, X. W.; Muller, U.; Yilmaz, B.; Feyen, M.; Gies, H.; Xiao, F. S.; De Vos, D.; Tatsumi, T.; Bao, X. H., Insights into the Topotactic Conversion Process from Layered Silicate RUB-36 to FER-type Zeolite by Layer Reassembly. *Chem. Mat.* **2013,** *25* (6), 840-847.
19. Verheyen, E.; Joos, L.; Van Havenbergh, K.; Breynaert, E.; Kasian, N.; Gobechiya, E.; Houthoofd, K.; Martineau, C.; Hinterstein, M.; Taulelle, F.; Van Speybroeck, V.; Waroquier, M.; Bals, S.; Van Tendeloo, G.; Kirschhock, C. E. A.; Martens, J. A., Design of zeolite by inverse sigma transformation. *Nat. Mater.* **2012,** *11* (12), 1059-1064.
20. Chlubná-Eliášová, P.; Tian, Y.; Pinar, A. B.; Kubů, M.; Morris, R. E.; Čejka, J., The ADOR mechanism for 3D-2D-3D transformation of germanosilicate IWW zeolite. *Angew. Chem.-Int. Edit.*, DOI: 10.1002/anie.201400600
21. Foster, M. D.; Treacy, M. M. J. A Database of Hypothetical Zeolite Structures. http://www.hypotheticalzeolites.net.
22. Pophale, R.; Cheeseman, P. A.; Deem, M. W., A database of new zeolite-like materials. *Phys. Chem. Chem. Phys.* **2011,** *13* (27), 12407-12412.
23. Majda, D.; Paz, F. A. A.; Friedrichs, O. D.; Foster, M. D.; Simperler, A.; Bell, R. G.; Klinowski, J., Hypothetical zeolitic frameworks: In search of potential heterogeneous catalysts. *J. Phys. Chem. C* **2008,** *112* (4), 1040-1047.
24. Li, Y.; Yu, J. H.; Xu, R. R., Criteria for Zeolite Frameworks Realizable for Target Synthesis. *Angew. Chem.-Int. Edit.* **2013,** *52* (6), 1673-1677.
25. Sanders, M. J.; Leslie, M.; Catlow, C. R. A., Interatomic Potentials for SiO2. *J. Chem. Soc.-Chem. Commun.* **1984,** (19), 1271-1273.
26. Schroder, K. P.; Sauer, J.; Leslie, M.; Catlow, C. R. A.; Thomas, J. M., Bridging Hydroxyl-Groups in Zeolitic Catalysts - a Computer-Simulation of Their Structure, Vibrational Properties and Acidity in Protonated Faujasites (H-Y Zeolites). *Chem. Phys. Lett.* **1992,** *188* (3-4), 320-325.
27. Koch, W.; Holthausen, M. C., *A Chemist's Guide to Density Functional Theory*. Wiley-WCH: 2001.
28. Perdew, J. P.; Burke, K.; Ernzerhof, M., Generalized gradient approximation made simple. *Phys. Rev. Lett.* **1996,** *77* (18), 3865-3868.
29. Lee, K.; Murray, E. D.; Kong, L. Z.; Lundqvist, B. I.; Langreth, D. C., Higher-accuracy van der Waals density functional. *Phys. Rev. B* **2010,** *82* (8), 4.
30. Gale, J. D., GULP: A computer program for the symmetry-adapted simulation of solids. *J. Chem. Soc.-Faraday Trans.* **1997,** *93* (4), 629-637.
31. Klimes, J.; Bowler, D. R.; Michaelides, A., Van der Waals density functionals applied to solids. *Phys. Rev. B* **2011,** *83* (19), 13.
32. Kresse, G.; Hafner, J., Abinitio Molecular-Dynamics for Liquid-Metals. *Phys. Rev. B* **1993,** *47* (1), 558-561.

33. Blochl, P. E., Projector Augmented-Wave Method. *Phys. Rev. B* **1994,** *50* (24), 17953-17979.
34. Corma, A.; Diaz-Cabanas, M. J.; Jorda, J. L.; Rey, F.; Sastre, G.; Strohmaier, K. G., A Zeolitic Structure (ITQ-34) with Connected 9-and 10-Ring Channels Obtained with Phosphonium Cations as Structure Directing Agents. *J. Am. Chem. Soc.* **2008,** *130* (49), 16482-+.
35. Blatov, V. A.; Ilyushin, G. D.; Proserpio, D. M., The Zeolite Conundrum: Why Are There so Many Hypothetical Zeolites and so Few Observed? A Possible Answer from the Zeolite-Type Frameworks Perceived As Packings of Tiles. *Chem. Mat.* **2013,** *25* (3), 412-424.
36. Sartbaeva, A.; Wells, S. A.; Treacy, M. M. J.; Thorpe, M. F., The flexibility window in zeolites. *Nat. Mater.* **2006,** *5* (12), 962-965.
37. Zwijnenburg, M. A.; Simperler, A.; Wells, S. A.; Bell, R. G., Tetrahedral distortion and energetic packing penalty in "zeolite" frameworks: Linked phenomena? *J. Phys. Chem. B* **2005,** *109* (31), 14783-14785.
38. MATLAB Release 2011a, T. M., Inc., Natick, Massachusetts, United States.
39. Treacy, M. M. J.; Foster, M. D.; Randall, K. H., An efficient method for determining zeolite vertex symbols. *Microporous Mesoporous Mat.* **2006,** *87* (3), 255-260.
40. Spek, A. L., Structure validation in chemical crystallography. *Acta Crystallogr. Sect. D-Biol. Crystallogr.* **2009,** *65*, 148-155.
41. Wheatley, P. S.; Chlubná-Eliášová, P.; Greer, H.; Zhou, W.; Seymour, V. R.; Dawson, D. M.; Ashbrook, S. E.; Pinar, A. B.; McCusker, L. B.; Opanasenko, M.; Čejka, J.; Morris, R. E., A zeolite with continuously tuneable porosity. *unpublished results*
42. Bruno, I. J.; Cole, J. C.; Edgington, P. R.; Kessler, M.; Macrae, C. F.; McCabe, P.; Pearson, J.; Taylor, R., New software for searching the Cambridge Structural Database and visualizing crystal structures. *Acta Crystallogr. Sect. B-Struct. Sci.* **2002,** *58*, 389-397.
43. Moliner, M.; Willhammar, T.; Wan, W.; Gonzalez, J.; Rey, F.; Jorda, J. L.; Zou, X. D.; Corma, A., Synthesis Design and Structure of a Multipore Zeolite with Interconnected 12- and 10-MR Channels. *J. Am. Chem. Soc.* **2012,** *134* (14), 6473-6478.

# Appendix A – Supplementary Data

**Table A1.** Objective function and energies during the optimization protocol for -D4R structures

| Zeolite | Objective function[a] [Å$^2$] | $FE_{opt1}$[b] [kJ/mol] | $FE_{sym1}$[b] [kJ/mol] | $FE_{opt2}$[b] [kJ/mol] | $FE_{sym2}$[b] [kJ/mol] |
|---|---|---|---|---|---|
| UTL | | | | | |
| -D4R(C2/m) | 0 | 9.1 | 9.1 | 9.1 | 9.1 |
| -D4R(Pm) | 15 | 11.7 | 11.7 | 11.7 | 11.7 |
| -D4R(P1) | 10 | 12.5 | | | |
| -D4R(Pm') | 25 | 14.7 | 14.7 | 14.7 | 14.7 |
| IWW | | | | | |
| -D4R(Pbam) | 0 | 11.0 | 11.0 | 11.0 | 11.0 |
| -D4R(C2/c) | 31 | 19.0 | 19.0 | 19.0 | 19.0 |
| -D4R(Aba2) | 51 | 22.3 | 22.3 | 22.3 | 22.3 |
| IWV | | | | | |
| -D4R(Fmmm) | 0 | 11.1 | 11.1 | 11.1 | 11.1 |
| -D4R(Cmm2) | 28 | 16.7 | 16.9 | 16.8 | 16.8 |
| -D4R(C2/m) | 38 | 21.2 | 21.5 | 21.2 | 21.2 |
| IWR | | | | | |
| -D4R($P1_{Cmmm}$) | 0 | 11.3 | | | |
| -D4R(C2/m) | 13 | 11.4 | 11.6 | 11.5 | 11.5 |
| -D4R(Cmmm) | 0 | 11.3 | 12.4 | 12.3 | 12.3 |
| -D4R(Fmmm) | 24 | 13.4 | 13.4 | 13.3 | 13.3 |
| ITH | | | | | |
| -D4R($P1_{Amm2}$) | 0 | 8.9 | | | |
| -D4R(Cm) | 5 | 9.4 | 9.5 | 9.4 | 9.4 |
| -D4R(Cm') | 6 | 9.8 | 10.7 | 9.7 | 9.7 |
| -D4R(Amm2) | 0 | 8.9 | 10.0 | 9.9 | 9.9 |
| ITR | | | | | |
| -D4R(P21/m) | 0; 0 | 8.3 | 8.3 | 8.3 | 8.3 |
| -D4R(P-1) | 0; 6 | 8.2 | 8.3 | 8.3 | 8.3 |
| -D4R(C2/m) | 0; 5 | 8.4 | 8.4 | 8.4 | 8.4 |
| -D4R(C2/m') | 0; 6 | 8.7 | 8.8 | 8.7 | 8.7 |

[a] Objective function defined in section 3.3.1. [b] These energies are dispersion-corrected PBE data, the dispersion contribution was counted as a difference of vdW-DF2 and PBE energy for the final structure. $FE_{sym2}$ ($FE_{opt1}$ for P1 structures) is equal to $FE_{DFT}$ data in Table 3.

**Table A2.** Objective function and energies during the optimization protocol for -S4R structures

| Zeolite | Objective function[a] [Å$^2$] | $FE_{opt1}$[b] [kJ/mol] | $FE_{sym1}$[b] [kJ/mol] | $FE_{opt2}$[b] [kJ/mol] | $FE_{sym2}$[b] [kJ/mol] |
|---|---|---|---|---|---|
| UTL | | | | | |
| -S4R(C2) | 5 | 11.2 | 11.2 | 11.2 | 11.2 |
| -S4R(P1) | 19 | 18.8 | | | |
| -S4R(Pm) | 30 | 18.8 | 18.8 | 18.8 | 18.8 |
| -S4R(P1') | 34 | 21.0 | | | |
| IWW | | | | | |
| -S4R(P1) | 21 | 11.6 | | | |
| -S4R(C2/c) | 34 | 16.1 | 16.1 | 16.1 | 16.1 |
| IWV | | | | | |
| -S4R(P1) | 11 | 10.3 | | | |
| IWR | | | | | |
| -S4R(C2/m) | 11 | 12.1 | 12.4 | 12.3 | 12.3 |
| -S4R(Cmcm) | 50 | 14.9 | 14.9 | 14.8 | 14.8 |
| -S4R(Immm) | 50 | 17.2 | 17.7 | 17.1 | 17.1 |
| ITH | | | | | |
| -S4R(Cmc21) | 25 | 9.3 | 9.3 | 9.3 | 9.3 |
| -S4R(Cm) | 25 | 9.5 | 9.4 | 9.4 | 9.4 |
| -S4R(P1) | 11 | 9.5 | | | |
| -S4R(Cm') | 24 | 9.5 | 9.6 | 9.6 | 9.6 |
| -S4R(Imm2) | 25 | 10.3 | 10.9 | 10.3 | 10.3 |
| -S4R(Cm'') | 32 | 10.8 | 10.7 | 10.7 | 10.7 |
| -S4R(Cm''') | 32 | 11.3 | 11.6 | 11.3 | 11.3 |
| -S4R(Cm'''') | 26 | 12.1 | 16.9 | 12.3 | 12.3 |
| ITR | | | | | |
| -S4R(Pnnm) | 25; 25 | 9.3 | 9.3 | 9.3 | 9.3 |
| -S4R(C2/c) | 11; 11 | 9.2 | 15.9 | 9.3 | 9.3 |
| -S4R(C2) | 11; 25 | 9.4 | 9.4 | 9.4 | 9.4 |
| -S4R(P-1) | 25; 25 | 9.5 | 9.5 | 9.5 | 9.5 |
| -S4R(Cm) | 11; 25 | 9.6 | 12.8 | 9.5 | 9.5 |
| -S4R(P1) | 11; 25 | 9.5 | | | |
| -S4R(P21) | 25; 25 | 9.6 | 9.7 | 9.7 | 9.7 |
| -S4R(P-1') | 25; 25 | 9.7 | 9.7 | 9.7 | 9.7 |
| -S4R(P-1'') | 11; 25 | 9.7 | 9.7 | 9.7 | 9.7 |

[a] Objective function defined in section 3.4.1. [b] These energies are dispersion-corrected PBE data, the dispersion contribution was counted as a difference of vdW-DF2 and PBE energy for the final structure. $FE_{sym2}$ ($FE_{opt1}$ for P1 structures) is equal to $FE_{DFT}$ data in Table 4.

**Table A3.** -D4R structures modeled by SLC potential

| Zeolite | Objective function[a] | $FE_{FF}$[b] | $FD_{FF}$[b] | Feasibility factor $\vartheta$[b] | LID criteria[b] | | | | |
|---|---|---|---|---|---|---|---|---|---|
| | [Å$^2$] | [kJ/mol] | [$10^{-3}$Å$^{-3}$] | | 1 | 2 | 3 | 4 | 5 |
| UTL | | | | | | | | | |
| -D4R(FF1)(C2/m) | 0 | 10.4 | 19.3 | 1.4 | 1 | 1 | 1 | 1 | 1 |
| -D4R(FF2)(Pm) | 15 | 12.5 | 20.2 | 1.0 | 1 | 1 | 1 | 1 | 1 |
| -D4R(FF3)(P1) | 10 | 14.0 | 19.8 | 1.7 | 0 | 1 | 1 | 0 | 1 |
| -D4R(FF4)(Pm') | 25 | 15.6 | 20.6 | 3.5 | 0 | 1 | 0 | 0 | 1 |
| IWW | | | | | | | | | |
| -D4R(FF1)(Pbam) | 0 | 12.3 | 19.1 | 0.2 | 1 | 1 | 1 | 1 | 1 |
| -D4R(FF2) | 56 | 18.7 | 21.0 | 6.2 | 0 | 1 | 0 | 0 | 1 |
| -D4R(FF3)(C2/c) | 31 | 21.9 | 21.0 | 8.4 | 0 | 1 | 0 | 0 | 0 |
| -D4R(FF4) | 81 | 22.8 | 21.9 | 9.9 | 0 | 1 | 0 | 0 | 0 |
| -D4R(FF5)(Aba2) | 51 | 25.1 | 21.8 | 11.4 | 0 | 1 | 0 | 0 | 0 |
| IWV | | | | | | | | | |
| -D4R(FF1)(Fmmm) | 0 | 10.6 | 19.9 | 0.7 | 1 | 1 | 1 | 1 | 1 |
| -D4R(FF2)(Cmm2) | 28 | 16.6 | 20.6 | 4.3 | 0 | 1 | 0 | 0 | 1 |
| -D4R(FF3)(C2/m) | 38 | 24.1 | 21.6 | 10.5 | 0 | 1 | 0 | 0 | 0 |
| IWR | | | | | | | | | |
| -D4R(FF1)(C2/m) | 13 | 14.1 | 18.8 | 0.7 | 1 | 1 | 1 | 1 | 1 |
| -D4R(FF2)(Cmmm) | 0 | 15.0 | 18.0 | 0.5 | 1 | 1 | 1 | 1 | 1 |
| -D4R(FF3)(Fmmm) | 24 | 17.8 | 18.9 | 3.5 | 1 | 1 | 1 | 1 | 0 |
| ITH | | | | | | | | | |
| -D4R(FF1)(Cm') | 6 | 10.5 | 20.6 | 0.1 | 1 | 1 | 1 | 1 | 1 |
| -D4R(FF2)(Amm2) | 0 | 11.2 | 20.4 | 0.3 | 1 | 1 | 1 | 1 | 1 |
| -D4R(FF3)(Cm) | 5 | 11.7 | 20.6 | 0.9 | 1 | 1 | 1 | 1 | 1 |
| ITR | | | | | | | | | |
| -D4R(FF1) | 5; 6 | 10.0 | 21.0 | 0.0 | 1 | 1 | 1 | 1 | 1 |
| -D4R(FF2)(P-1) | 0; 6 | 10.0 | 20.8 | 0.2 | 1 | 1 | 1 | 1 | 1 |
| -D4R(FF3) | 6; 6 | 10.0 | 20.7 | 0.2 | 1 | 1 | 1 | 1 | 1 |
| -D4R(FF4)(P21/m) | 0; 0 | 10.0 | 20.5 | 0.4 | 1 | 1 | 1 | 1 | 1 |
| -D4R(FF5)(C2/m) | 0; 5 | 10.1 | 20.7 | 0.2 | 1 | 1 | 1 | 1 | 1 |
| -D4R(FF6)(C2/m') | 0; 6 | 10.6 | 20.8 | 0.2 | 1 | 1 | 1 | 1 | 1 |
| -D4R(FF7) | 6; 6 | 10.6 | 20.8 | 0.3 | 1 | 1 | 1 | 1 | 1 |
| -D4R(FF8) | 6; 6 | 11.2 | 20.6 | 0.5 | 1 | 1 | 1 | 1 | 1 |
| -D4R(FF9) | 5; 6 | 11.5 | 20.7 | 0.8 | 1 | 1 | 1 | 1 | 1 |
| -D4R(FF10) | 6; 6 | 11.6 | 20.8 | 1.0 | 1 | 1 | 1 | 1 | 1 |

[a] Objective function defined in section 3.3.1. [b] For definition see section 3.2.

**Table A4.** -S4R structures modeled by SLC potential

| Zeolite | Objective function[a] | $FE_{FF}$[b] | $FD_{FF}$[b] | Feasibility factor ϑ[b] | LID criteria[b] | | | | |
|---|---|---|---|---|---|---|---|---|---|
| | [Å$^2$] | [kJ/mol] | [$10^{-3}$Å$^{-3}$] | | 1 | 2 | 3 | 4 | 5 |
| UTL | | | | | | | | | |
| -S4R(FF1)(C2) | 5 | 13.8 | 17.8 | 0.5 | 1 | 1 | 1 | 1 | 1 |
| -S4R(FF2)(P1) | 19 | 22.2 | 18.9 | 6.5 | 0 | 1 | 0 | 0 | 1 |
| -S4R(FF3)(Pm) | 30 | 23.3 | 19.3 | 7.7 | 0 | 1 | 0 | 0 | 1 |
| -S4R(FF4)(P1') | 34 | 24.1 | 19.7 | 8.7 | 0 | 1 | 0 | 0 | 1 |
| -S4R(FF5) | 54 | 25.9 | 20.0 | 10.2 | 0 | 0 | 0 | 0 | 0 |
| -S4R(FF6) | 83 | 27.6 | 22.2 | 13.6 | 0 | 0 | 0 | 0 | 0 |
| -S4R(FF7) | 58 | 27.7 | 21.6 | 13.1 | 0 | 1 | 0 | 0 | 0 |
| -S4R(FF8) | 44 | 29.3 | 20.8 | 13.3 | 0 | 1 | 0 | 0 | 0 |
| -S4R(FF9) | 44 | 29.4 | 20.7 | 13.3 | 0 | 1 | 0 | 0 | 0 |
| -S4R(FF10) | 69 | 33.0 | 21.5 | 16.7 | 0 | 0 | 0 | 0 | 0 |
| IWW | | | | | | | | | |
| -S4R(FF1)(P1) | 21 | 13.5 | 19.1 | 0.6 | 1 | 1 | 1 | 1 | 1 |
| -S4R(FF2)(C2/c) | 34 | 19.2 | 19.3 | 4.8 | 0 | 1 | 0 | 0 | 1 |
| -S4R(FF3) | 78 | 21.3 | 19.4 | 6.4 | 0 | 1 | 0 | 0 | 1 |
| -S4R(FF4) | 41 | 22.4 | 19.8 | 7.5 | 0 | 1 | 0 | 0 | 1 |
| -S4R(FF5) | 166 | 24.0 | 19.7 | 8.6 | 0 | 1 | 0 | 0 | 0 |
| -S4R(FF6) | 159 | 26.9 | 19.9 | 10.7 | 0 | 1 | 0 | 0 | 0 |
| -S4R(FF7) | 281 | 37.0 | 20.6 | 18.6 | 0 | 0 | 0 | 0 | 0 |
| IWV | | | | | | | | | |
| -S4R(FF1)(P1) | 11 | 12.5 | 17.8 | 1.4 | 1 | 1 | 1 | 1 | 1 |
| -S4R(FF2) | 58 | 21.3 | 19.6 | 6.6 | 0 | 1 | 1 | 0 | 1 |
| -S4R(FF3) | 58 | 22.4 | 19.6 | 7.4 | 0 | 1 | 0 | 0 | 0 |
| -S4R(FF4) | 58 | 22.9 | 19.4 | 7.5 | 0 | 1 | 0 | 0 | 0 |
| -S4R(FF5) | 72 | 24.5 | 20.4 | 9.6 | 0 | 1 | 0 | 0 | 0 |
| -S4R(FF6) | 58 | 26.4 | 19.4 | 9.9 | 0 | 1 | 0 | 0 | 0 |
| -S4R(FF7) | 96 | 28.3 | 21.3 | 13.1 | 0 | 1 | 0 | 0 | 0 |
| -S4R(FF8) | 120 | 32.1 | 22.0 | 16.6 | 0 | 1 | 0 | 0 | 0 |
| IWR | | | | | | | | | |
| -S4R(FF1)(C2/m) | 11 | 16.2 | 18.0 | 1.4 | 1 | 1 | 1 | 1 | 1 |
| -S4R(FF2)(Cmcm) | 50 | 18.4 | 19.6 | 4.6 | 1 | 1 | 1 | 0 | 0 |
| -S4R(FF3)(Immm) | 50 | 21.1 | 19.3 | 6.2 | 1 | 1 | 1 | 1 | 0 |
| -S4R(FF4) | 34 | 21.9 | 18.1 | 5.6 | 1 | 1 | 1 | 0 | 1 |
| -S4R(FF5) | 54 | 22.7 | 18.7 | 6.7 | 1 | 1 | 1 | 0 | 0 |
| -S4R(FF6) | 58 | 25.5 | 18.1 | 8.1 | 0 | 1 | 0 | 0 | 0 |
| -S4R(FF7) | 58 | 25.5 | 18.1 | 8.1 | 0 | 1 | 0 | 0 | 0 |
| -S4R(FF8) | 58 | 27.6 | 18.3 | 9.6 | 0 | 1 | 0 | 0 | 0 |
| -S4R(FF9) | 50 | 29.9 | 19.1 | 12.0 | 0 | 1 | 0 | 0 | 0 |
| -S4R(FF10) | 74 | 33.3 | 19.0 | 14.4 | 0 | 0 | 0 | 0 | 0 |
| -S4R(FF11) | 54 | 38.3 | 18.6 | 17.5 | 0 | 0 | 0 | 0 | 0 |
| -S4R(FF12) | 50 | 38.6 | 19.1 | 18.2 | 0 | 0 | 0 | 0 | 0 |
| -S4R(FF13) | 90 | 39.3 | 20.2 | 19.8 | 0 | 0 | 0 | 0 | 0 |
| -S4R(FF14) | 50 | 41.3 | 19.9 | 20.8 | 0 | 0 | 0 | 0 | 0 |
| -S4R(FF15) | 58 | 48.5 | 18.1 | 24.1 | 0 | 0 | 0 | 0 | 0 |
| -S4R(FF16) | 58 | 49.0 | 18.3 | 24.6 | 0 | 0 | 0 | 0 | 0 |
| -S4R(FF17) | 58 | 50.2 | 18.3 | 25.5 | 0 | 0 | 0 | 0 | 0 |
| ITH | | | | | | | | | |
| -S4R(FF1)(P1) | 11 | 11.1 | 20.2 | 0.0 | 1 | 1 | 1 | 1 | 1 |
| -S4R(FF2)(Cmc21) | 25 | 11.2 | 19.8 | 0.3 | 1 | 1 | 1 | 1 | 1 |
| -S4R(FF3)(Cm) | 25 | 11.4 | 19.7 | 0.2 | 1 | 1 | 1 | 1 | 1 |
| -S4R(FF4)(Cm') | 24 | 12.0 | 19.7 | 0.2 | 1 | 1 | 1 | 1 | 1 |
| -S4R(FF5)(Imm2) | 25 | 12.4 | 19.7 | 0.4 | 1 | 1 | 1 | 1 | 1 |
| -S4R(FF6)(Cm") | 32 | 13.6 | 19.8 | 1.4 | 1 | 1 | 1 | 1 | 1 |
| -S4R(FF7)(Cm"') | 32 | 14.0 | 19.8 | 1.6 | 1 | 1 | 1 | 1 | 1 |
| -S4R(FF8)(Cm"") | 26 | 14.7 | 20.1 | 2.4 | 1 | 1 | 1 | 1 | 1 |
| -S4R(FF9) | 38 | 16.6 | 19.6 | 3.2 | 1 | 1 | 1 | 0 | 1 |

| Zeolite | Objective function[a] | $FE_{FF}$[b] | $FD_{FF}$[b] | Feasibility factor ϑ[b] | LID criteria[b] | | | | |
|---|---|---|---|---|---|---|---|---|---|
| | [Å$^2$] | [kJ/mol] | [$10^{-3}$Å$^{-3}$] | | 1 | 2 | 3 | 4 | 5 |
| -S4R(FF10) | 25 | 17.1 | 19.9 | 3.9 | 0 | 1 | 1 | 0 | 1 |
| -S4R(FF11) | 25 | 17.6 | 19.9 | 4.2 | 0 | 1 | 1 | 0 | 1 |
| -S4R(FF12) | 32 | 18.1 | 20.0 | 4.7 | 1 | 1 | 1 | 0 | 1 |
| -S4R(FF13) | 32 | 18.1 | 20.0 | 4.7 | 0 | 1 | 1 | 0 | 1 |
| -S4R(FF14) | 40 | 21.3 | 20.0 | 7.0 | 0 | 1 | 0 | 0 | 1 |
| -S4R(FF15) | 39 | 22.8 | 19.7 | 7.7 | 0 | 1 | 0 | 0 | 1 |
| -S4R(FF16) | 39 | 25.2 | 19.9 | 9.6 | 0 | 1 | 0 | 0 | 1 |
| -S4R(FF17) | 39 | 25.9 | 20.1 | 10.3 | 0 | 1 | 0 | 0 | 0 |
| -S4R(FF18) | 39 | 27.3 | 20.1 | 11.3 | 0 | 1 | 0 | 0 | 0 |
| -S4R(FF19) | 37 | 27.8 | 19.5 | 11.0 | 0 | 1 | 0 | 0 | 1 |
| -S4R(FF20) | 39 | 30.4 | 19.9 | 13.2 | 0 | 1 | 0 | 0 | 0 |
| -S4R(FF21) | 39 | 30.9 | 19.9 | 13.6 | 0 | 1 | 0 | 0 | 0 |
| -S4R(FF22) | 41 | 32.2 | 20.3 | 14.8 | 0 | 1 | 0 | 0 | 0 |
| ITR | | | | | | | | | |
| -S4R(FF1)(C2/c) | 11; 11 | 10.7 | 20.2 | 0.2 | 1 | 1 | 1 | 1 | 1 |
| -S4R(FF2)(Pnnm) | 25; 25 | 11.3 | 19.8 | 0.2 | 1 | 1 | 1 | 1 | 1 |
| -S4R(FF3)(P-1) | 11; 25 | 11.3 | 19.9 | 0.1 | 1 | 1 | 1 | 1 | 1 |
| -S4R(FF4)(C2) | 11; 25 | 11.3 | 19.9 | 0.1 | 1 | 1 | 1 | 1 | 1 |
| -S4R(FF5)(Cm) | 11; 25 | 11.4 | 19.9 | 0.1 | 1 | 1 | 1 | 1 | 1 |
| -S4R(FF6)(P-1") | 11; 25 | 11.6 | 20.0 | 0.1 | 1 | 1 | 1 | 1 | 1 |
| -S4R(FF7)(P21) | 25; 25 | 11.6 | 19.7 | 0.1 | 1 | 1 | 1 | 1 | 1 |
| -S4R(FF8)(P1) | 11; 24 | 11.6 | 19.8 | 0.1 | 1 | 1 | 1 | 1 | 1 |
| -S4R(FF9)(P-1') | 25; 25 | 11.6 | 19.8 | 0.0 | 1 | 1 | 1 | 1 | 1 |
| -S4R(FF10) | 11; 25 | 11.9 | 19.9 | 0.3 | 1 | 1 | 1 | 1 | 1 |
| -S4R(FF11) | 24; 25 | 11.9 | 19.7 | 0.1 | 1 | 1 | 1 | 1 | 1 |
| -S4R(FF12) | 25; 25 | 12.0 | 19.7 | 0.1 | 1 | 1 | 1 | 1 | 1 |
| -S4R(FF13) | 24; 24 | 12.0 | 19.7 | 0.2 | 1 | 1 | 1 | 1 | 1 |
| -S4R(FF14) | 11; 38 | 12.2 | 19.6 | 0.2 | 1 | 1 | 1 | 1 | 1 |
| -S4R(FF15) | 11; 32 | 12.3 | 19.9 | 0.5 | 1 | 1 | 1 | 1 | 1 |
| -S4R(FF16) | 11; 32 | 12.3 | 19.9 | 0.5 | 1 | 1 | 1 | 1 | 1 |
| -S4R(FF17) | 11; 38 | 12.3 | 19.7 | 0.4 | 1 | 1 | 1 | 1 | 1 |
| -S4R(FF18) | 25; 32 | 12.6 | 19.8 | 0.6 | 1 | 1 | 1 | 1 | 1 |
| -S4R(FF19) | 11; 32 | 12.6 | 19.9 | 0.8 | 1 | 1 | 1 | 1 | 1 |
| -S4R(FF20) | 11; 32 | 12.7 | 19.9 | 0.8 | 1 | 1 | 1 | 1 | 1 |
| -S4R(FF21) | 25; 32 | 12.9 | 19.8 | 0.9 | 1 | 1 | 1 | 1 | 1 |
| -S4R(FF22) | 25; 32 | 12.9 | 19.7 | 0.8 | 1 | 1 | 1 | 1 | 1 |
| -S4R(FF23) | 24; 25 | 13.0 | 19.8 | 0.9 | 1 | 1 | 1 | 0 | 1 |
| -S4R(FF24) | 11; 38 | 13.0 | 19.7 | 0.9 | 1 | 1 | 1 | 1 | 1 |
| -S4R(FF25) | 24; 25 | 13.1 | 19.8 | 1.0 | 1 | 1 | 1 | 1 | 1 |
| -S4R(FF26) | 25; 32 | 13.2 | 19.8 | 1.0 | 1 | 1 | 1 | 0 | 1 |
| -S4R(FF27) | 11; 26 | 13.2 | 20.0 | 1.3 | 1 | 1 | 1 | 1 | 1 |
| -S4R(FF28) | 24; 25 | 13.2 | 19.7 | 1.1 | 1 | 1 | 1 | 0 | 1 |
| -S4R(FF29) | 25; 26 | 13.3 | 19.9 | 1.2 | 1 | 1 | 1 | 1 | 1 |
| -S4R(FF30) | 24; 25 | 13.4 | 19.7 | 1.2 | 1 | 1 | 1 | 0 | 1 |
| -S4R(FF31) | 24; 26 | 13.4 | 19.9 | 1.4 | 1 | 1 | 1 | 1 | 1 |
| -S4R(FF32) | 32; 32 | 13.6 | 19.8 | 1.4 | 1 | 1 | 1 | 1 | 1 |
| -S4R(FF33) | 24; 32 | 13.6 | 19.8 | 1.4 | 1 | 1 | 1 | 0 | 1 |
| -S4R(FF34) | 11; 39 | 13.7 | 19.9 | 1.6 | 1 | 1 | 1 | 0 | 1 |
| -S4R(FF35) | 11; 40 | 13.7 | 19.9 | 1.6 | 1 | 1 | 1 | 1 | 1 |
| -S4R(FF36) | 25; 25 | 13.8 | 19.9 | 1.6 | 1 | 1 | 1 | 0 | 1 |
| -S4R(FF37) | 32; 32 | 13.8 | 19.8 | 1.5 | 1 | 1 | 1 | 1 | 1 |
| -S4R(FF38) | 25; 25 | 13.8 | 19.8 | 1.6 | 1 | 1 | 1 | 0 | 1 |
| -S4R(FF39) | 25; 38 | 13.9 | 19.6 | 1.4 | 1 | 1 | 1 | 0 | 1 |
| -S4R(FF40) | 24; 32 | 13.9 | 19.8 | 1.6 | 1 | 1 | 1 | 0 | 1 |
| -S4R(FF41) | 25; 25 | 13.9 | 19.8 | 1.6 | 1 | 1 | 1 | 0 | 1 |
| -S4R(FF42) | 24; 32 | 13.9 | 19.8 | 1.6 | 1 | 1 | 1 | 0 | 1 |

| Zeolite | Objective function[a] | $FE_{FF}$[b] | $FD_{FF}$[b] | Feasibility factor ϑ[b] | LID criteria[b] | | | | |
|---|---|---|---|---|---|---|---|---|---|
| | [Å$^2$] | [kJ/mol] | [$10^{-3}$Å$^{-3}$] | | 1 | 2 | 3 | 4 | 5 |
| -S4R(FF43) | 25; 25 | 13.9 | 19.8 | 1.7 | 1 | 1 | 1 | 0 | 1 |
| -S4R(FF44) | 11; 39 | 13.9 | 19.8 | 1.7 | 1 | 1 | 1 | 1 | 1 |
| -S4R(FF45) | 11; 39 | 14.0 | 20.0 | 1.8 | 1 | 1 | 1 | 0 | 1 |
| -S4R(FF46) | 24; 25 | 14.0 | 19.8 | 1.7 | 1 | 1 | 1 | 0 | 1 |
| -S4R(FF47) | 25; 25 | 14.0 | 19.8 | 1.7 | 1 | 1 | 1 | 0 | 1 |
| -S4R(FF48) | 25; 25 | 14.1 | 19.8 | 1.7 | 1 | 1 | 1 | 0 | 1 |
| -S4R(FF49) | 24; 32 | 14.1 | 19.8 | 1.7 | 1 | 1 | 1 | 0 | 1 |
| -S4R(FF50) | 32; 32 | 14.1 | 19.8 | 1.7 | 1 | 1 | 1 | 1 | 1 |
| -S4R(FF51) | 25; 39 | 14.2 | 19.7 | 1.7 | 1 | 1 | 1 | 1 | 1 |
| -S4R(FF52) | 25; 25 | 14.2 | 19.8 | 1.9 | 1 | 1 | 1 | 0 | 1 |
| -S4R(FF53) | 25; 39 | 14.3 | 19.8 | 1.8 | 1 | 1 | 1 | 1 | 1 |
| -S4R(FF54) | 11; 39 | 14.4 | 19.8 | 2.0 | 1 | 1 | 1 | 0 | 1 |
| -S4R(FF55) | 24; 38 | 14.4 | 19.6 | 1.8 | 1 | 1 | 1 | 0 | 1 |
| -S4R(FF56) | 25; 26 | 14.5 | 20.0 | 2.2 | 1 | 1 | 1 | 0 | 1 |
| -S4R(FF57) | 25; 32 | 14.6 | 19.8 | 2.1 | 1 | 1 | 1 | 0 | 1 |
| -S4R(FF58) | 25; 26 | 14.6 | 20.0 | 2.3 | 1 | 1 | 1 | 0 | 1 |
| -S4R(FF59) | 24; 38 | 14.6 | 19.6 | 1.8 | 1 | 1 | 1 | 0 | 1 |
| -S4R(FF60) | 25; 39 | 14.6 | 19.9 | 2.2 | 1 | 1 | 1 | 1 | 1 |
| -S4R(FF61) | 25; 32 | 14.6 | 19.8 | 2.1 | 1 | 1 | 1 | 0 | 1 |
| -S4R(FF62) | 25; 32 | 14.6 | 19.8 | 2.1 | 1 | 1 | 1 | 0 | 1 |
| -S4R(FF63) | 25; 32 | 14.6 | 19.8 | 2.2 | 1 | 1 | 1 | 0 | 1 |
| -S4R(FF64) | 11; 39 | 14.7 | 19.9 | 2.2 | 1 | 1 | 1 | 1 | 1 |
| -S4R(FF65) | 25; 39 | 14.7 | 19.8 | 2.2 | 1 | 1 | 1 | 1 | 1 |
| -S4R(FF66) | 25; 32 | 14.7 | 19.8 | 2.2 | 1 | 1 | 1 | 0 | 1 |
| -S4R(FF67) | 25; 32 | 14.8 | 19.8 | 2.3 | 1 | 1 | 1 | 0 | 1 |
| -S4R(FF68) | 25; 32 | 14.8 | 19.9 | 2.4 | 1 | 1 | 1 | 0 | 1 |
| -S4R(FF69) | 25; 26 | 14.9 | 19.9 | 2.4 | 1 | 1 | 1 | 0 | 1 |
| -S4R(FF70) | 26; 26 | 14.9 | 20.1 | 2.6 | 1 | 1 | 1 | 1 | 1 |
| -S4R(FF71) | 25; 32 | 14.9 | 19.9 | 2.4 | 1 | 1 | 1 | 0 | 1 |
| -S4R(FF72) | 25; 26 | 14.9 | 19.9 | 2.4 | 1 | 1 | 1 | 0 | 1 |
| -S4R(FF73) | 25; 38 | 14.9 | 19.6 | 2.1 | 1 | 1 | 1 | 1 | 1 |
| -S4R(FF74) | 25; 38 | 14.9 | 19.6 | 2.1 | 1 | 1 | 1 | 1 | 1 |
| -S4R(FF75) | 25; 32 | 14.9 | 19.8 | 2.3 | 1 | 1 | 1 | 0 | 1 |
| -S4R(FF76) | 25; 32 | 14.9 | 19.8 | 2.4 | 1 | 1 | 1 | 0 | 1 |
| -S4R(FF77) | 25; 32 | 15.0 | 19.9 | 2.4 | 1 | 1 | 1 | 0 | 1 |
| -S4R(FF78) | 25; 32 | 15.0 | 19.9 | 2.4 | 1 | 1 | 1 | 0 | 1 |
| -S4R(FF79) | 25; 38 | 15.0 | 19.6 | 2.2 | 1 | 1 | 1 | 0 | 1 |
| -S4R(FF80) | 25; 32 | 15.0 | 19.8 | 2.4 | 1 | 1 | 1 | 0 | 1 |
| -S4R(FF81) | 25; 32 | 15.0 | 19.9 | 2.4 | 1 | 1 | 1 | 0 | 1 |
| -S4R(FF82) | 25; 32 | 15.1 | 19.9 | 2.5 | 1 | 1 | 1 | 0 | 1 |
| -S4R(FF83) | 25; 38 | 15.1 | 19.6 | 2.2 | 1 | 1 | 1 | 1 | 1 |
| -S4R(FF84) | 25; 32 | 15.1 | 19.9 | 2.5 | 1 | 1 | 1 | 0 | 1 |
| -S4R(FF85) | 25; 38 | 15.1 | 19.6 | 2.3 | 1 | 1 | 1 | 0 | 1 |
| -S4R(FF86) | 25; 38 | 15.3 | 19.7 | 2.5 | 1 | 1 | 1 | 0 | 1 |
| -S4R(FF87) | 26; 32 | 15.3 | 19.9 | 2.7 | 1 | 1 | 1 | 0 | 1 |
| -S4R(FF88) | 26; 32 | 15.4 | 19.9 | 2.8 | 1 | 1 | 1 | 0 | 1 |
| -S4R(FF89) | 26; 32 | 15.4 | 20.0 | 2.8 | 1 | 1 | 1 | 0 | 1 |
| -S4R(FF90) | 25; 38 | 15.4 | 19.7 | 2.6 | 1 | 1 | 1 | 0 | 1 |
| -S4R(FF91) | 11; 41 | 15.5 | 20.0 | 2.9 | 1 | 1 | 1 | 1 | 1 |
| -S4R(FF92) | 26; 32 | 15.5 | 19.9 | 2.9 | 1 | 1 | 1 | 0 | 1 |
| -S4R(FF93) | 25; 38 | 15.5 | 19.7 | 2.6 | 1 | 1 | 1 | 0 | 1 |
| -S4R(FF94) | 32; 32 | 15.5 | 19.9 | 2.8 | 1 | 1 | 1 | 0 | 1 |
| -S4R(FF95) | 32; 32 | 15.6 | 19.9 | 2.8 | 1 | 1 | 1 | 0 | 1 |
| -S4R(FF96) | 25; 38 | 15.6 | 19.7 | 2.7 | 1 | 1 | 1 | 0 | 1 |
| -S4R(FF97) | 32; 32 | 15.6 | 19.8 | 2.9 | 1 | 1 | 1 | 0 | 1 |
| -S4R(FF98) | 32; 32 | 15.7 | 19.9 | 3.0 | 1 | 1 | 1 | 0 | 1 |

| Zeolite | Objective function[a] | $FE_{FF}$[b] | $FD_{FF}$[b] | Feasibility factor ϑ[b] | LID criteria[b] | | | | |
|---|---|---|---|---|---|---|---|---|---|
| | [Å$^2$] | [kJ/mol] | [$10^{-3}$Å$^{-3}$] | | 1 | 2 | 3 | 4 | 5 |
| -S4R(FF99) | 25; 38 | 16.2 | 19.7 | 3.2 | 1 | 1 | 1 | 0 | 1 |
| -S4R(FF100) | 26; 38 | 16.2 | 19.8 | 3.2 | 1 | 1 | 1 | 0 | 1 |
| -S4R(FF101) | 25; 40 | 16.2 | 19.9 | 3.3 | 1 | 1 | 1 | 0 | 1 |
| -S4R(FF102) | 25; 38 | 16.3 | 19.7 | 3.2 | 1 | 1 | 1 | 0 | 1 |
| -S4R(FF103) | 25; 39 | 16.3 | 19.8 | 3.3 | 1 | 1 | 1 | 0 | 1 |
| -S4R(FF104) | 24; 40 | 16.4 | 19.8 | 3.4 | 1 | 1 | 1 | 0 | 1 |
| -S4R(FF105) | 32; 38 | 16.4 | 19.7 | 3.3 | 1 | 1 | 1 | 0 | 1 |
| -S4R(FF106) | 25; 26 | 16.4 | 20.0 | 3.5 | 0 | 1 | 1 | 0 | 1 |
| -S4R(FF107) | 25; 39 | 16.4 | 19.8 | 3.3 | 1 | 1 | 1 | 0 | 1 |
| -S4R(FF108) | 32; 38 | 16.5 | 19.7 | 3.3 | 1 | 1 | 1 | 0 | 1 |
| -S4R(FF109) | 25; 39 | 16.5 | 19.7 | 3.3 | 1 | 1 | 1 | 0 | 1 |
| -S4R(FF110) | 25; 39 | 16.5 | 19.8 | 3.4 | 1 | 1 | 1 | 0 | 1 |
| -S4R(FF111) | 25; 39 | 16.5 | 19.8 | 3.4 | 1 | 1 | 1 | 0 | 1 |
| -S4R(FF112) | 25; 38 | 16.5 | 19.7 | 3.3 | 1 | 1 | 1 | 0 | 1 |
| -S4R(FF113) | 26; 38 | 16.5 | 19.8 | 3.5 | 1 | 1 | 1 | 0 | 1 |
| -S4R(FF114) | 32; 38 | 16.6 | 19.7 | 3.4 | 1 | 1 | 1 | 0 | 1 |
| -S4R(FF115) | 38; 38 | 16.6 | 19.6 | 3.2 | 1 | 1 | 1 | 0 | 1 |
| -S4R(FF116) | 25; 39 | 16.6 | 19.7 | 3.4 | 1 | 1 | 1 | 0 | 1 |
| -S4R(FF117) | 25; 39 | 16.6 | 19.8 | 3.5 | 1 | 1 | 1 | 0 | 1 |
| -S4R(FF118) | 38; 38 | 16.6 | 19.6 | 3.3 | 1 | 1 | 1 | 1 | 1 |
| -S4R(FF119) | 32; 38 | 16.7 | 19.7 | 3.5 | 1 | 1 | 1 | 0 | 1 |
| -S4R(FF120) | 25; 39 | 16.7 | 19.8 | 3.6 | 1 | 1 | 1 | 0 | 1 |
| -S4R(FF121) | 25; 25 | 16.7 | 20.0 | 3.8 | 0 | 1 | 1 | 0 | 1 |
| -S4R(FF122) | 25; 39 | 16.8 | 19.7 | 3.6 | 1 | 1 | 1 | 0 | 1 |
| -S4R(FF123) | 25; 25 | 16.8 | 19.9 | 3.8 | 0 | 1 | 1 | 0 | 1 |
| -S4R(FF124) | 25; 38 | 16.9 | 19.7 | 3.6 | 1 | 1 | 1 | 0 | 1 |
| -S4R(FF125) | 25; 38 | 17.0 | 19.6 | 3.6 | 0 | 1 | 1 | 0 | 1 |
| -S4R(FF126) | 25; 25 | 17.0 | 19.9 | 3.9 | 0 | 1 | 1 | 0 | 1 |
| -S4R(FF127) | 25; 39 | 17.1 | 19.8 | 3.8 | 1 | 1 | 1 | 0 | 1 |
| -S4R(FF128) | 25; 38 | 17.1 | 19.6 | 3.7 | 0 | 1 | 1 | 0 | 1 |
| -S4R(FF129) | 25; 39 | 17.2 | 19.8 | 3.9 | 1 | 1 | 1 | 0 | 1 |
| -S4R(FF130) | 25; 39 | 17.2 | 19.8 | 3.9 | 0 | 1 | 1 | 0 | 1 |
| -S4R(FF131) | 32; 32 | 17.2 | 19.9 | 4.0 | 0 | 1 | 1 | 0 | 1 |
| -S4R(FF132) | 25; 25 | 17.2 | 19.9 | 4.0 | 0 | 1 | 1 | 0 | 1 |
| -S4R(FF133) | 25; 32 | 17.3 | 19.9 | 4.1 | 0 | 1 | 1 | 0 | 1 |
| -S4R(FF134) | 25; 39 | 17.3 | 19.8 | 4.0 | 0 | 1 | 1 | 0 | 1 |
| -S4R(FF135) | 25; 32 | 17.4 | 19.9 | 4.1 | 0 | 1 | 1 | 0 | 1 |
| -S4R(FF136) | 32; 32 | 17.4 | 19.9 | 4.1 | 0 | 1 | 1 | 0 | 1 |
| -S4R(FF137) | 25; 40 | 17.4 | 19.9 | 4.1 | 0 | 1 | 1 | 0 | 1 |
| -S4R(FF138) | 25; 32 | 17.4 | 19.9 | 4.2 | 0 | 1 | 1 | 0 | 1 |
| -S4R(FF139) | 25; 40 | 17.5 | 19.9 | 4.2 | 0 | 1 | 1 | 0 | 1 |
| -S4R(FF140) | 32; 32 | 17.5 | 19.9 | 4.2 | 0 | 1 | 1 | 0 | 1 |
| -S4R(FF141) | 32; 38 | 17.5 | 19.7 | 4.0 | 1 | 1 | 1 | 0 | 1 |
| -S4R(FF142) | 32; 38 | 17.5 | 19.8 | 4.1 | 1 | 1 | 1 | 0 | 1 |
| -S4R(FF143) | 25; 32 | 17.6 | 19.9 | 4.2 | 0 | 1 | 1 | 0 | 1 |
| -S4R(FF144) | 25; 39 | 17.7 | 19.7 | 4.1 | 0 | 1 | 1 | 0 | 1 |
| -S4R(FF145) | 25; 40 | 17.7 | 19.9 | 4.3 | 0 | 1 | 1 | 0 | 1 |
| -S4R(FF146) | 32; 32 | 17.8 | 19.9 | 4.4 | 0 | 1 | 1 | 0 | 1 |
| -S4R(FF147) | 25; 40 | 17.8 | 19.9 | 4.4 | 0 | 1 | 1 | 0 | 1 |
| -S4R(FF148) | 26; 40 | 17.9 | 20.0 | 4.6 | 0 | 1 | 1 | 0 | 1 |
| -S4R(FF149) | 32; 38 | 17.9 | 19.7 | 4.3 | 0 | 1 | 1 | 0 | 1 |
| -S4R(FF150) | 32; 32 | 18.0 | 19.9 | 4.6 | 0 | 1 | 1 | 0 | 1 |
| -S4R(FF151) | 32; 32 | 18.0 | 19.9 | 4.6 | 0 | 1 | 1 | 0 | 1 |
| -S4R(FF152) | 32; 38 | 18.0 | 19.7 | 4.4 | 0 | 1 | 1 | 0 | 1 |
| -S4R(FF153) | 32; 39 | 18.1 | 20.0 | 4.8 | 0 | 1 | 1 | 0 | 1 |
| -S4R(FF154) | 32; 39 | 18.1 | 19.9 | 4.7 | 1 | 1 | 1 | 0 | 1 |

| Zeolite | Objective function[a] | $FE_{FF}$[b] | $FD_{FF}$[b] | Feasibility factor ϑ[b] | LID criteria[b] | | | | |
|---|---|---|---|---|---|---|---|---|---|
| | [Å$^2$] | [kJ/mol] | [$10^{-3}$Å$^{-3}$] | | 1 | 2 | 3 | 4 | 5 |
| -S4R(FF155) | 24; 32 | 18.2 | 19.9 | 4.7 | 0 | 1 | 1 | 0 | 1 |
| -S4R(FF156) | 32; 40 | 18.2 | 19.9 | 4.7 | 0 | 1 | 1 | 0 | 1 |
| -S4R(FF157) | 32; 39 | 18.2 | 20.0 | 4.8 | 0 | 1 | 1 | 0 | 1 |
| -S4R(FF158) | 26; 38 | 18.3 | 20.0 | 4.9 | 0 | 1 | 1 | 0 | 1 |
| -S4R(FF159) | 24; 32 | 18.3 | 19.9 | 4.8 | 0 | 1 | 1 | 0 | 1 |
| -S4R(FF160) | 32; 40 | 18.3 | 19.9 | 4.8 | 0 | 1 | 1 | 0 | 1 |
| -S4R(FF161) | 32; 40 | 18.4 | 19.9 | 4.9 | 0 | 1 | 1 | 0 | 1 |
| -S4R(FF162) | 32; 39 | 18.4 | 19.9 | 4.9 | 0 | 1 | 1 | 0 | 1 |
| -S4R(FF163) | 25; 41 | 18.4 | 20.0 | 5.0 | 0 | 1 | 0 | 0 | 1 |
| -S4R(FF164) | 32; 40 | 18.5 | 19.9 | 4.9 | 0 | 1 | 1 | 0 | 1 |
| -S4R(FF165) | 24; 39 | 18.5 | 20.0 | 5.0 | 0 | 1 | 1 | 0 | 1 |
| -S4R(FF166) | 26; 38 | 18.5 | 20.0 | 5.0 | 0 | 1 | 1 | 0 | 1 |
| -S4R(FF167) | 25; 41 | 18.6 | 20.0 | 5.1 | 0 | 1 | 0 | 0 | 1 |
| -S4R(FF168) | 24; 32 | 18.6 | 19.9 | 5.0 | 0 | 1 | 1 | 0 | 1 |
| -S4R(FF169) | 25; 41 | 18.6 | 20.0 | 5.2 | 0 | 1 | 0 | 0 | 1 |
| -S4R(FF170) | 25; 41 | 18.6 | 20.0 | 5.1 | 0 | 1 | 0 | 0 | 1 |
| -S4R(FF171) | 24; 40 | 18.7 | 19.9 | 5.1 | 0 | 1 | 1 | 0 | 1 |
| -S4R(FF172) | 25; 39 | 18.8 | 19.8 | 5.0 | 0 | 1 | 0 | 0 | 1 |
| -S4R(FF173) | 25; 41 | 18.8 | 20.0 | 5.2 | 0 | 1 | 0 | 0 | 1 |
| -S4R(FF174) | 38; 38 | 18.8 | 19.7 | 4.9 | 0 | 1 | 1 | 0 | 1 |
| -S4R(FF175) | 38; 40 | 18.8 | 19.8 | 5.0 | 0 | 1 | 0 | 0 | 1 |
| -S4R(FF176) | 24; 26 | 18.9 | 20.2 | 5.5 | 0 | 1 | 0 | 0 | 1 |
| -S4R(FF177) | 24; 32 | 19.0 | 19.9 | 5.2 | 0 | 1 | 1 | 0 | 1 |
| -S4R(FF178) | 25; 40 | 19.0 | 19.9 | 5.2 | 0 | 1 | 0 | 0 | 1 |
| -S4R(FF179) | 24; 39 | 19.0 | 19.9 | 5.2 | 0 | 1 | 1 | 0 | 1 |
| -S4R(FF180) | 24; 38 | 19.0 | 19.6 | 4.9 | 1 | 1 | 1 | 0 | 1 |
| -S4R(FF181) | 25; 39 | 19.0 | 19.8 | 5.2 | 0 | 1 | 0 | 0 | 1 |
| -S4R(FF182) | 38; 39 | 19.1 | 19.7 | 5.2 | 0 | 1 | 0 | 0 | 1 |
| -S4R(FF183) | 24; 39 | 19.1 | 19.9 | 5.3 | 0 | 1 | 1 | 0 | 1 |
| -S4R(FF184) | 24; 39 | 19.2 | 19.9 | 5.3 | 0 | 1 | 1 | 0 | 1 |
| -S4R(FF185) | 24; 38 | 19.2 | 19.7 | 5.2 | 0 | 1 | 1 | 0 | 1 |
| -S4R(FF186) | 25; 39 | 19.2 | 19.7 | 5.2 | 0 | 1 | 0 | 0 | 1 |
| -S4R(FF187) | 25; 39 | 19.2 | 19.8 | 5.3 | 0 | 1 | 0 | 0 | 1 |
| -S4R(FF188) | 32; 38 | 19.3 | 19.8 | 5.3 | 0 | 1 | 1 | 0 | 1 |
| -S4R(FF189) | 24; 39 | 19.3 | 19.9 | 5.4 | 0 | 1 | 1 | 0 | 1 |
| -S4R(FF190) | 38; 39 | 19.3 | 19.7 | 5.3 | 0 | 1 | 0 | 0 | 1 |
| -S4R(FF191) | 32; 38 | 19.3 | 19.8 | 5.4 | 0 | 1 | 1 | 0 | 1 |
| -S4R(FF192) | 38; 39 | 19.3 | 19.7 | 5.3 | 0 | 1 | 0 | 0 | 1 |
| -S4R(FF193) | 32; 38 | 19.3 | 19.8 | 5.4 | 0 | 1 | 1 | 0 | 1 |
| -S4R(FF194) | 32; 38 | 19.4 | 19.8 | 5.4 | 0 | 1 | 1 | 0 | 1 |
| -S4R(FF195) | 38; 39 | 19.4 | 19.8 | 5.4 | 0 | 1 | 0 | 0 | 1 |
| -S4R(FF196) | 32; 32 | 19.4 | 20.0 | 5.7 | 0 | 1 | 0 | 0 | 1 |
| -S4R(FF197) | 38; 39 | 19.4 | 19.7 | 5.4 | 0 | 1 | 0 | 0 | 1 |
| -S4R(FF198) | 32; 32 | 19.5 | 20.0 | 5.7 | 0 | 1 | 1 | 0 | 1 |
| -S4R(FF199) | 26; 32 | 19.6 | 20.2 | 5.9 | 0 | 1 | 0 | 0 | 1 |
| -S4R(FF200) | 24; 24 | 19.6 | 19.7 | 5.5 | 0 | 1 | 1 | 0 | 1 |
| -S4R(FF201) | 32; 32 | 19.6 | 20.0 | 5.8 | 0 | 1 | 0 | 0 | 1 |
| -S4R(FF202) | 32; 39 | 19.7 | 20.0 | 5.8 | 0 | 1 | 1 | 0 | 1 |
| -S4R(FF203) | 32; 39 | 19.8 | 20.0 | 5.9 | 0 | 1 | 1 | 0 | 1 |
| -S4R(FF204) | 38; 39 | 19.8 | 20.0 | 6.0 | 0 | 1 | 0 | 0 | 0 |
| -S4R(FF205) | 26; 32 | 19.9 | 20.1 | 6.1 | 0 | 1 | 0 | 0 | 1 |
| -S4R(FF206) | 26; 32 | 19.9 | 20.1 | 6.1 | 0 | 1 | 0 | 0 | 1 |
| -S4R(FF207) | 32; 39 | 19.9 | 20.0 | 6.0 | 0 | 1 | 0 | 0 | 1 |
| -S4R(FF208) | 32; 32 | 20.0 | 19.8 | 5.9 | 0 | 1 | 1 | 0 | 1 |
| -S4R(FF209) | 32; 39 | 20.2 | 20.1 | 6.3 | 0 | 1 | 0 | 0 | 1 |
| -S4R(FF210) | 26; 32 | 20.2 | 20.1 | 6.3 | 0 | 1 | 0 | 0 | 1 |

| Zeolite | Objective function[a] | $FE_{FF}$[b] | $FD_{FF}$[b] | Feasibility factor ϑ[b] | LID criteria[b] | | | | |
|---|---|---|---|---|---|---|---|---|---|
| | [Å$^2$] | [kJ/mol] | [$10^{-3}$Å$^{-3}$] | | 1 | 2 | 3 | 4 | 5 |
| -S4R(FF211) | 32; 32 | 20.2 | 19.9 | 6.1 | 0 | 1 | 1 | 0 | 1 |
| -S4R(FF212) | 32; 32 | 20.2 | 19.9 | 6.1 | 0 | 1 | 0 | 0 | 1 |
| -S4R(FF213) | 26; 39 | 20.4 | 20.1 | 6.4 | 0 | 1 | 0 | 0 | 1 |
| -S4R(FF214) | 26; 39 | 20.4 | 20.1 | 6.5 | 0 | 1 | 0 | 0 | 1 |
| -S4R(FF215) | 26; 39 | 20.5 | 20.1 | 6.4 | 0 | 1 | 0 | 0 | 1 |
| -S4R(FF216) | 32; 39 | 20.5 | 20.0 | 6.4 | 0 | 1 | 0 | 0 | 1 |
| -S4R(FF217) | 26; 39 | 20.6 | 20.1 | 6.6 | 0 | 1 | 0 | 0 | 1 |
| -S4R(FF218) | 24; 41 | 20.6 | 20.3 | 6.7 | 0 | 1 | 0 | 0 | 1 |
| -S4R(FF219) | 32; 38 | 20.6 | 19.7 | 6.2 | 0 | 1 | 1 | 0 | 1 |
| -S4R(FF220) | 32; 39 | 20.7 | 20.0 | 6.5 | 0 | 1 | 0 | 0 | 1 |
| -S4R(FF221) | 32; 38 | 20.7 | 19.7 | 6.3 | 0 | 1 | 0 | 0 | 1 |
| -S4R(FF222) | 32; 38 | 20.7 | 19.7 | 6.2 | 0 | 1 | 1 | 0 | 1 |
| -S4R(FF223) | 26; 39 | 20.7 | 20.1 | 6.7 | 0 | 1 | 0 | 0 | 1 |
| -S4R(FF224) | 32; 38 | 20.8 | 19.7 | 6.4 | 0 | 1 | 0 | 0 | 1 |
| -S4R(FF225) | 40; 40 | 20.9 | 20.0 | 6.7 | 0 | 1 | 0 | 0 | 1 |
| -S4R(FF226) | 38; 40 | 20.9 | 20.0 | 6.7 | 0 | 1 | 0 | 0 | 0 |
| -S4R(FF227) | 32; 39 | 20.9 | 20.0 | 6.7 | 0 | 1 | 0 | 0 | 1 |
| -S4R(FF228) | 38; 38 | 20.9 | 19.5 | 6.2 | 0 | 1 | 1 | 0 | 1 |
| -S4R(FF229) | 24; 39 | 21.0 | 19.8 | 6.5 | 0 | 1 | 1 | 0 | 1 |
| -S4R(FF230) | 32; 39 | 21.1 | 19.9 | 6.7 | 0 | 1 | 0 | 0 | 1 |
| -S4R(FF231) | 32; 39 | 21.1 | 19.9 | 6.7 | 0 | 1 | 0 | 0 | 1 |
| -S4R(FF232) | 32; 39 | 21.1 | 20.0 | 6.9 | 0 | 1 | 0 | 0 | 1 |
| -S4R(FF233) | 32; 39 | 21.2 | 19.9 | 6.8 | 0 | 1 | 0 | 0 | 1 |
| -S4R(FF234) | 26; 39 | 21.3 | 20.0 | 6.9 | 0 | 1 | 0 | 0 | 1 |
| -S4R(FF235) | 32; 39 | 21.3 | 19.9 | 6.8 | 0 | 1 | 0 | 0 | 1 |
| -S4R(FF236) | 38; 39 | 21.3 | 19.8 | 6.8 | 0 | 1 | 0 | 0 | 1 |
| -S4R(FF237) | 26; 40 | 21.4 | 20.0 | 7.1 | 0 | 1 | 0 | 0 | 1 |
| -S4R(FF238) | 38; 39 | 21.4 | 19.9 | 6.9 | 0 | 1 | 0 | 0 | 1 |
| -S4R(FF239) | 32; 39 | 21.4 | 19.9 | 6.9 | 0 | 1 | 0 | 0 | 1 |
| -S4R(FF240) | 38; 39 | 21.4 | 19.8 | 6.9 | 0 | 1 | 0 | 0 | 1 |
| -S4R(FF241) | 32; 39 | 21.5 | 19.9 | 7.0 | 0 | 1 | 0 | 0 | 1 |
| -S4R(FF242) | 38; 39 | 21.6 | 19.9 | 7.1 | 0 | 1 | 0 | 0 | 1 |
| -S4R(FF243) | 32; 39 | 21.6 | 19.9 | 7.1 | 0 | 1 | 0 | 0 | 1 |
| -S4R(FF244) | 32; 39 | 21.6 | 19.9 | 7.1 | 0 | 1 | 0 | 0 | 1 |
| -S4R(FF245) | 26; 26 | 21.8 | 20.3 | 7.6 | 0 | 1 | 0 | 0 | 1 |
| -S4R(FF246) | 38; 41 | 21.8 | 19.9 | 7.3 | 0 | 1 | 0 | 0 | 1 |
| -S4R(FF247) | 32; 40 | 21.9 | 20.1 | 7.5 | 0 | 1 | 0 | 0 | 1 |
| -S4R(FF248) | 38; 40 | 22.0 | 19.8 | 7.2 | 0 | 1 | 0 | 0 | 1 |
| -S4R(FF249) | 32; 40 | 22.0 | 20.1 | 7.5 | 0 | 1 | 0 | 0 | 1 |
| -S4R(FF250) | 38; 38 | 22.1 | 19.7 | 7.3 | 0 | 1 | 0 | 0 | 1 |
| -S4R(FF251) | 32; 40 | 22.6 | 20.0 | 7.9 | 0 | 1 | 0 | 0 | 1 |
| -S4R(FF252) | 39; 40 | 22.7 | 20.1 | 8.1 | 0 | 1 | 0 | 0 | 0 |
| -S4R(FF253) | 32; 41 | 22.8 | 20.2 | 8.2 | 0 | 1 | 0 | 0 | 1 |
| -S4R(FF254) | 39; 40 | 23.0 | 20.0 | 8.1 | 0 | 1 | 0 | 0 | 1 |
| -S4R(FF255) | 32; 40 | 23.1 | 20.0 | 8.2 | 0 | 1 | 0 | 0 | 1 |
| -S4R(FF256) | 32; 39 | 23.1 | 19.9 | 8.1 | 0 | 1 | 0 | 0 | 1 |
| -S4R(FF257) | 32; 41 | 23.1 | 20.2 | 8.4 | 0 | 1 | 0 | 0 | 1 |
| -S4R(FF258) | 32; 32 | 23.2 | 19.9 | 8.1 | 0 | 1 | 0 | 0 | 1 |
| -S4R(FF259) | 32; 32 | 23.2 | 19.8 | 8.2 | 0 | 1 | 0 | 0 | 1 |
| -S4R(FF260) | 32; 32 | 23.3 | 19.9 | 8.2 | 0 | 1 | 0 | 0 | 1 |
| -S4R(FF261) | 39; 40 | 23.3 | 20.1 | 8.5 | 0 | 1 | 0 | 0 | 0 |
| -S4R(FF262) | 39; 40 | 23.3 | 20.1 | 8.4 | 0 | 1 | 0 | 0 | 0 |
| -S4R(FF263) | 38; 40 | 23.3 | 19.9 | 8.3 | 0 | 1 | 0 | 0 | 0 |
| -S4R(FF264) | 38; 41 | 23.3 | 20.2 | 8.6 | 0 | 1 | 0 | 0 | 0 |
| -S4R(FF265) | 26; 41 | 23.4 | 20.2 | 8.6 | 0 | 1 | 0 | 0 | 1 |
| -S4R(FF266) | 39; 40 | 23.5 | 20.1 | 8.6 | 0 | 1 | 0 | 0 | 0 |

| Zeolite | Objective function[a] | $FE_{FF}$[b] | $FD_{FF}$[b] | Feasibility factor ϑ[b] | LID criteria[b] | | | | |
|---|---|---|---|---|---|---|---|---|---|
| | [Å$^2$] | [kJ/mol] | [$10^{-3}$Å$^{-3}$] | | 1 | 2 | 3 | 4 | 5 |
| -S4R(FF267) | 32; 39 | 23.5 | 19.9 | 8.4 | 0 | 1 | 0 | 0 | 1 |
| -S4R(FF268) | 32; 41 | 23.5 | 20.2 | 8.7 | 0 | 1 | 0 | 0 | 1 |
| -S4R(FF269) | 32; 39 | 23.6 | 20.0 | 8.6 | 0 | 1 | 0 | 0 | 1 |
| -S4R(FF270) | 39; 40 | 23.6 | 20.0 | 8.6 | 0 | 1 | 0 | 0 | 0 |
| -S4R(FF271) | 32; 41 | 23.7 | 20.2 | 8.8 | 0 | 1 | 0 | 0 | 1 |
| -S4R(FF272) | 32; 39 | 23.8 | 20.0 | 8.7 | 0 | 1 | 0 | 0 | 1 |
| -S4R(FF273) | 38; 39 | 23.8 | 19.7 | 8.4 | 0 | 1 | 0 | 0 | 1 |
| -S4R(FF274) | 38; 38 | 24.1 | 19.4 | 8.4 | 0 | 1 | 0 | 0 | 1 |
| -S4R(FF275) | 39; 39 | 25.0 | 20.0 | 9.5 | 0 | 1 | 0 | 0 | 1 |
| -S4R(FF276) | 39; 39 | 25.2 | 20.0 | 9.8 | 0 | 1 | 0 | 0 | 0 |
| -S4R(FF277) | 39; 39 | 25.7 | 20.2 | 10.2 | 0 | 1 | 0 | 0 | 0 |
| -S4R(FF278) | 40; 41 | 26.4 | 20.1 | 10.7 | 0 | 1 | 0 | 0 | 0 |
| -S4R(FF279) | 39; 39 | 26.5 | 20.2 | 10.8 | 0 | 1 | 0 | 0 | 0 |
| -S4R(FF280) | 38; 41 | 27.3 | 20.3 | 11.5 | 0 | 1 | 0 | 0 | 0 |
| -S4R(FF281) | 40; 40 | 27.6 | 20.0 | 11.4 | 0 | 1 | 0 | 0 | 0 |
| -S4R(FF282) | 39; 39 | 28.0 | 19.9 | 11.5 | 0 | 1 | 0 | 0 | 0 |
| -S4R(FF283) | 38; 39 | 28.3 | 20.0 | 11.8 | 0 | 1 | 0 | 0 | 0 |
| -S4R(FF284) | 38; 39 | 28.3 | 19.9 | 11.8 | 0 | 1 | 0 | 0 | 0 |
| -S4R(FF285) | 39; 39 | 28.5 | 20.0 | 12.0 | 0 | 1 | 0 | 0 | 0 |
| -S4R(FF286) | 39; 39 | 28.5 | 20.1 | 12.2 | 0 | 1 | 0 | 0 | 0 |
| -S4R(FF287) | 39; 39 | 28.6 | 20.0 | 12.1 | 0 | 1 | 0 | 0 | 0 |
| -S4R(FF288) | 38; 39 | 28.8 | 19.9 | 12.1 | 0 | 1 | 0 | 0 | 0 |
| -S4R(FF289) | 38; 39 | 28.8 | 19.9 | 12.1 | 0 | 1 | 0 | 0 | 0 |
| -S4R(FF290) | 39; 39 | 29.0 | 20.0 | 12.4 | 0 | 1 | 0 | 0 | 0 |
| -S4R(FF291) | 39; 39 | 29.2 | 20.0 | 12.5 | 0 | 1 | 0 | 0 | 0 |
| -S4R(FF292) | 39; 41 | 29.3 | 20.2 | 12.8 | 0 | 1 | 0 | 0 | 0 |
| -S4R(FF293) | 38; 39 | 29.3 | 19.9 | 12.5 | 0 | 1 | 0 | 0 | 0 |
| -S4R(FF294) | 39; 41 | 29.3 | 20.1 | 12.7 | 0 | 1 | 0 | 0 | 0 |
| -S4R(FF295) | 39; 39 | 29.4 | 20.0 | 12.7 | 0 | 1 | 0 | 0 | 0 |
| -S4R(FF296) | 39; 41 | 29.5 | 20.2 | 12.9 | 0 | 1 | 0 | 0 | 0 |
| -S4R(FF297) | 39; 41 | 29.6 | 20.2 | 12.9 | 0 | 1 | 0 | 0 | 0 |
| -S4R(FF298) | 39; 41 | 30.4 | 20.1 | 13.4 | 0 | 1 | 0 | 0 | 0 |
| -S4R(FF299) | 38; 38 | 30.7 | 19.7 | 13.2 | 0 | 1 | 0 | 0 | 0 |
| -S4R(FF300) | 39; 39 | 32.1 | 20.0 | 14.5 | 0 | 1 | 0 | 0 | 0 |
| -S4R(FF301) | 39; 39 | 32.2 | 20.0 | 14.6 | 0 | 1 | 0 | 0 | 0 |
| -S4R(FF302) | 41; 41 | 32.2 | 20.1 | 14.8 | 0 | 1 | 0 | 0 | 0 |
| -S4R(FF303) | 39; 39 | 32.4 | 19.8 | 14.6 | 0 | 0 | 0 | 0 | 0 |
| -S4R(FF304) | 39; 39 | 32.5 | 20.2 | 15.0 | 0 | 0 | 0 | 0 | 0 |

[a] Objective function defined in section 3.4.1. [b] For definition see section 3.2.

# Appendix B – CD Content

DFT and FF optimized structures are on the attached CD. It also contains the powder diffraction patterns for the DFT-optimized structures and some of the MATLAB codes used in this work. The code for evaluating the vertex symbols (evalvs.m) was written by Ota Bludský (published with his permission), all other codes were written by Michal Trachta.

MATLAB codes:

- csvs.m – find unique CS/VS characteristics
- lidanalysis.m – code for LID analysis
- upravgeom.m – code used for preoptimization

(Other attached functions are necessary for running these three functions)